

1 **The Effects of Global Change upon United States Air Quality**

2
3 R. Gonzalez-Abraham^{1*}, J. Avise^{1,2}, S. H. Chung¹, B. Lamb¹, E. P. Salathé, Jr³, C. G.
4 Nolte⁴, D. Loughlin⁴, A. Guenther^{5**}, C. Wiedinmyer⁵, T. Duhl⁵, Y. Zhang⁵, D. G. Streets⁶

5
6
7 1. *Washington State University, Pullman, Washington, USA*

8 * Now at ~~*the Molina Center for Strategic Studies in Energy and the Environment, La*~~
9 ~~*Jolla, California*~~*Portland State University, Portland, Oregon USA*

10 2. *California Air Resources Board, Sacramento, California, USA*

11 3. *University of Washington, Seattle, Washington, USA*

12 4. *Environmental Protection Agency, Research Triangle Park, North Carolina, USA*

13 5. *National Center for Atmospheric Research, Boulder, Colorado, USA*

14 ** Now at Pacific Northwest National Laboratory, Richland, Washington, USA

15 6. *Argonne National Laboratory, Argonne, Illinois, USA*

16
17

18 **Correspondence to R. Gonzalez-Abraham**
19 **(rodrigoga@mce2.org or rodrigo@pdx.edu)**

20 **Abstract**

21 To understand more fully the effects of global changes on ambient concentrations
22 of ozone and particulate matter with aerodynamic diameter smaller than 2.5 μm ($\text{PM}_{2.5}$)
23 in the US, we conducted a comprehensive modeling effort to evaluate explicitly the effects
24 of changes in climate, biogenic emissions, land use, and global/regional anthropogenic
25 emissions on ozone and $\text{PM}_{2.5}$ concentrations and composition. Results from the
26 ECHAM5 global climate model driven with the A1B emission scenario from the
27 Intergovernmental Panel on Climate Change (IPCC) were downscaled using the Weather
28 Research and Forecasting (WRF) model to provide regional meteorological fields. We
29 developed air quality simulations using the Community Multiscale Air Quality Model
30 (CMAQ) chemical transport model for two nested domains with 220 km and 36 km
31 horizontal grid cell resolution for a semi-hemispheric domain and a continental United
32 States (US) domain, respectively. The semi-hemispheric domain was used to evaluate
33 the impact of projected [Asian–global](#) emissions changes on US air quality. WRF
34 meteorological fields were used to calculate current (2000s) and future (2050s) biogenic
35 emissions using the Model of Emissions of Gases and Aerosols from Nature (MEGAN).
36 For the semi-hemispheric domain CMAQ simulations, present-day global emissions
37 inventories were used and projected to the 2050s based on the IPCC A1B scenario.
38 Regional anthropogenic emissions were obtained from the US Environmental Protection
39 Agency National Emission Inventory 2002 (EPA NEI2002) and projected to the future
40 using the MARKet ALlocation (MARKAL) energy system model assuming a business as
41 usual scenario that extends current decade emission regulations through 2050. Our

42 results suggest that daily maximum 8 hour average ozone (DM8O) concentrations will
43 increase in a range between 2 to 12 parts per billion (ppb) across most of the continental
44 US, ~~with t~~The highest increase occurs in the South, Central, and Midwest regions of the
45 US, due to increases in temperature, enhanced biogenic emissions, and changes in land
46 use. ~~In the western US, the model predicts an average increase of 21-6 ppb in DM8O~~
47 ~~due to projected increase in global emissions in Asia of ozone precursors, particularly from~~
48 Asia. The effects of these factors are only partially offset by reductions in DM8O
49 associated with decreasing US anthropogenic emissions. Increases in PM_{2.5} levels
50 between 42 and 104 $\mu\text{g m}^{-3}$ in the Northeast, Southeast, Midwest and South regions are
51 mostly a result of increase in primary anthropogenic particulate matter (PM), enhanced
52 biogenic emissions and land use changes. ~~Little change in PM_{2.5} in the Central,~~
53 ~~Northwest, and Southwest regions was found, even when PM precursors are reduced~~
54 ~~with regulatory curtailment.~~ Changes in ~~temperature, relative humidity, and~~ boundary
55 conditions shift the composition but do not alter overall simulated PM_{2.5} mass
56 concentrations.

57 1. Introduction

58 Despite extensive efforts to reduce anthropogenic emissions, air pollution
59 continues to be a public health issue in the United States (EPA, 2010). Elevated
60 concentrations of pollutants in the troposphere, such as ozone (O₃) and particulate matter
61 ~~(PM)~~,_{2.5} degrade air quality and have been associated with, among other things, increasing
62 human respiratory diseases in urban areas (WHO, 2005),₁ and in the case of PM, with low
63 birth weights across the world (Dadvand et al., 2012).

64 High concentrations of tropospheric ~~ozone~~-O₃ and ~~particulate~~-PM matter with
65 aerodynamic diameter smaller than 2.5 μm (PM_{2.5}) are caused by a combination of
66 adverse meteorological conditions and the atmospheric emissions of their primary
67 precursors. While regulatory controls are expected to reduce emissions of many emitted
68 pollutants in the United States (US) in the future, the negative effects of global climate
69 change may offset the positive effects of such reductions. Furthermore, global emissions
70 of greenhouse gases and other pollutant precursors are projected to increase (IPCC,
71 2007). Moreover, recent research has provided evidence of increasing long-range
72 transport of ~~ozone~~-O₃ and PM_{2.5} precursors from Asia and their influence over the western
73 US. (Lelieveld and Dentener, 2000; Wuebbles et al., 2007; Cooper et al., 2010, Zhang et
74 al., 2010; Ambrose et al., 2011; Cooper et al., 2012, WMO, 2012, Lin et al., 2012).

75 In the United States, regulations and technological changes in the transportation
76 and energy sectors are projected to reduce regional atmospheric pollutants in the future
77 (Loughlin et al., 2011). However, the interplay between climate change, increasing global

78 emissions, and intercontinental transport pose challenges that air quality managers will
79 have to address in order to maintain regional air quality standards (Ravishankara et al.,
80 2012). To provide a foundation for building effective management strategies and public
81 policies in a changing global environment, modeling approaches that link global changes
82 with regional air quality are required. The general approach has been to use output from
83 general circulation models (GCMs) to drive regional climate models (RCMs) and regional
84 or global chemical transport models (CTMs/GTMs; Giorgi and Meleux, 2007; Jacob and
85 Winner, 2009).

86 This downscaling approach has been used in a variety of studies in Europe,
87 Canada, and Asia [at different time scales of climate change](#) (e.g., Liao et al., 2006 [\[2000](#)
88 [to 2100\]](#); Langner et al., 2005 [\[2000 to 2060\]](#); Forkel and Knoche, 2006 [\[2990 to 2030\]](#);
89 Meleux et al., 2007 [\[1975 to 1985\]](#); Kunkel et al., 2007 [\[1990 to 2090\]](#); Lin et al., 2008
90 [\[2000 to 2100\]](#); Spracklen et al., 2009 [\[2000 to 2050\]](#); Kelly et al., 2012 [\[2000's to 2050's\]](#)).
91 These investigations based the global emissions on future anthropogenic emissions
92 scenarios developed from the Intergovernmental Panel on Climate Change (IPCC)
93 assessment reports ~~[projected to 2050's, 2080 and 2100](#)~~. Despite the differences in
94 emission scenarios, [time scales](#), modeling frameworks and future climate realizations,
95 increases in ozone concentrations on the order of 2 to 10 ppb [in polluted regions](#) were
96 consistently predicted from these studies as a result of climate change alone. By contrast,
97 there is little consistency among the model predictions of climate change effects on
98 ~~[particulate matter \(PM\)](#)~~[PM](#) (Jacob et al, 2009; Dawson et al., 2013).

99 In the US, a combined effort between the [Environmental Protection Agency](#) and
100 the academic community resulted in a set of modeling studies that adopted a variety of
101 modeling methods (Hogrefe et al., 2004; Leung and Gustafson, 2005; Liang et al., 2006;
102 Steiner et al., 2006; Tagaris et al., 2007; Liao et al., 2006; [Racherla and Adams, 2006,](#)
103 [2008](#); Tao et al., 2007; Huang et al., 2007, 2008; Nolte et al., 2008; Wu et al, 2008a,
104 2008b; Chen et al, 2009b; Avise et al., 2009; [Dawson et al., 2009](#)). These US
105 investigations based their current and future climate realizations on the results of GCMs
106 using the various IPCC emissions scenarios (IPCC, 2007) [projected to the 2050's](#). In
107 some of the studies, the global climate realizations were subsequently downscaled to a
108 higher resolution using the PSU (Pennsylvania State University)/NCAR (National Center
109 for Atmospheric Research) Mesoscale Model version 5 (MM5; Grell et al., 1994) to
110 horizontal resolutions that ranged from 90 km to 36 km. Many of these studies based their
111 analysis on the effects of climate change on summer air quality in the [Contiguous](#)
112 [Continental US \(CONUS\)](#). In summary, despite the differences in modeling elements, all
113 studies found ~~an~~ increases in [daily the summer average of the daily](#) maximum ~~summer~~
114 [8-hour average](#) ozone concentrations [over large regions of the simulated CONUS domain](#)
115 on the order of 2 to 8 ppb ~~for the simulated CONUS domain~~ (Weaver et al., 2009), ~~but~~
116 [with regional variations](#). In contrast, PM concentrations showed changes between $\pm 0.1 \mu\text{g}$
117 m^{-3} to $\pm 1 \mu\text{g} \text{m}^{-3}$, with little consistency between studies, including the sign of the
118 differences ([Day and Pandis, 2015; Trail et al., 2014;](#) Jacob and Winner, 2009).

119 It is important to note that variations between modeling frameworks did result in
120 very diverse regional patterns of key weather drivers for ozone and PM formation. Thus,

121 while most of the studies mentioned above ~~found~~ projected an average increase in ozone
122 concentrations for the simulated domains, reductions or insignificant changes in certain
123 regions of the domain were also simulated. Generally, temperature and solar radiation
124 reaching the surface were the major meteorological drivers for regional ozone
125 concentrations. For PM concentrations, most of the studies found a direct link between
126 changes in precipitation and relative humidity and changes in PM concentrations (Liao et
127 al., 2006; Unger et al., 2006; Racherla and Adams 2006, Tagaris et al., 2007; Avise et
128 al., 2009; Chen et al., 2009b). Nevertheless, the direct impacts of changes in
129 meteorological conditions are not the only factors of change for ozone and PM
130 concentrations. Changes in emissions of biogenic volatile organic compounds (BVOCs),
131 due to climate and land cover change, and the treatment of isoprene nitrates in the
132 chemical mechanism were found to be a key factor in the regional variability of ozone and
133 PM, particularly in areas of the southeastern US (Jacob and Winner, 2009; Weaver et al.,
134 2009).

135 In this work, we present a continuation of the work described by Avise et al. (2009)
136 and Chen et al. (2009a, b), who downscaled the Parallel Climate Model (PCM;
137 Washington et al., 2000) and MOZART (Model for OZone And Related chemical Tracers;
138 Horowitz, 2006) global model output for the A2 IPCC scenario using MM5 and the
139 Community Multi-scale Air Quality Model (CMAQ; Byun and Schere, 2006) to simulate
140 current and future air quality in the US. For this update, we implemented a semi-
141 hemispheric domain for the Weather Research and Forecasting (WRF) mesoscale
142 meteorological model (<http://www.wrf-model.org>) and CMAQ simulations in lieu of using

143 MOZART output for chemical boundary conditions for our CONUS CMAQ simulations.
144 We used the ECHAM5 global climate model (Roeckner et al., 1999, 2003) output for the
145 A1B scenario to drive these simulations for two decadal periods: the current decade from
146 1995–2004 and the future decade 2045–2054. In presenting our results, we follow the
147 attribution approach described in Avise et al. (2009), where the separate and combined
148 effects of changes in climate, US anthropogenic emissions, global anthropogenic
149 emissions and biogenic emissions due to changes in regional meteorology and land use
150 are investigated. Ideally, this framework should include feedback from changes in
151 atmospheric chemistry to the climate system (Raes et al., 2010). However, due to the
152 computational requirements of an on-line approach, we did not incorporate feedback
153 between the atmospheric chemistry and transport simulations from the CTM to the RCM.
154 Furthermore, despite the observed sensitivity of tropospheric ozone to regional emissions
155 and global burden of methane (Zhang et al., 2011; Fiore et al., 2008; Wu et al., 2008a;
156 Nolte et al., 2008; Fiore et al., 2006), in this work, we do not address the [potential direct](#)
157 [contribution effect of emissions of methane in the air quality simulations.](#)

158 In Section 2, we provide an overview of the modeling framework and emissions
159 scenarios. Evaluation of the model performance for the climate simulations and results of
160 the changes in meteorological fields are presented in Section 3. Assessment of air quality
161 changes and the individual and combined effects from changes in model components are
162 presented in Section 4. Finally, we present a summary of the results and conclusions in
163 Section 5.

164 2. Methodology

165 2.1 General Framework

166 Results from the global climate model ECHAM5 under the IPCC Special Report
167 on Emissions Scenarios (SRES) A1B scenario (Nakicenovic et al., 2000) were
168 downscaled using the WRF model separately to a semi-hemispheric (S-HEM) 220 km
169 domain and nested CONUS domains of 108 km (not shown) and 36 km (Figure 1).
170 Although, it has been suggested that periods of 10 to 30 years are required to fully
171 determine climatological conditions (Andersson and Engardt, 2010), the fact that
172 emission inventories can substantially change from one decade to the next suggests that
173 using five to ten year periods for air quality assessment is more appropriate. Thus, five
174 representative summers (June-July-August; with May as a spin-up period) for the present
175 (1995 to 2004) and the future (2045 to 2054) decades were selected. Ranked in terms of
176 their CONUS-mean maximum temperature of the year, the summers of the warmest and
177 coldest years, as well as the second, fifth and seventh warmest years in each decade
178 were selected for CMAQ simulations. Comparison of the meteorological conditions of
179 these five ~~selected~~~~chosen~~ summers to those of the full decades is presented in section
180 3.1. These five representative summers (June-July-August; with May as a spin-up period)
181 for the present and future periods were processed with the Meteorology-Chemistry
182 Interface Processor v3.4.1 (MCIP; Otte and Pleim, 2010) for the S-HEM and 36 km
183 CONUS domains. Meteorological fields generated from MCIP for both domains were
184 used to estimate biogenic emissions using the Model of Emissions of Gases and Aerosols
185 from Nature v2.04 (MEGANv2.04; Guenther et al., 2006) and to calculate the temporal
186 profiles within the Sparse Matrix Operator Kernel Emissions (SMOKE) v2.7

187 (<http://www.smoke-model.org>). With the elements described above, a framework to
188 perform air quality simulations using the Community Multiscale Air Quality Model (CMAQ
189 v4.7; Foley et al., 2010) was created. The overall schematic for the modeling system is
190 shown in Figure 2.

191 **2.2 Climate and Meteorology**

192 The regional weather model WRF includes advanced representations of land-
193 surface dynamics and cloud microphysics to simulate complex interactions between
194 atmospheric processes and the land surface characteristics. Detailed descriptions of
195 WRF can be found at <http://wrf-model.org> and a discussion of its range of regional climate
196 modeling applications ~~can be found in~~ is detailed by Leung et al. (2006). In this experiment,
197 WRF was used to downscale the ECHAM5 output for both the S-HEM and 108/36 km
198 CONUS domains. The model was applied with 31 vertical levels and a vertical resolution
199 of ~ 40 – 100 m throughout the boundary layer with the model top fixed at 50 mb. Details
200 of the model setup and a discussion of the results are reported by Salathé et al. (2010),
201 Zhang et al. (2009, 2012), and Duliére (2011, 2013).

202 **2.3 Current and Future Biogenic Emissions and Land Use Changes**

203 The MEGANv2.04 biogenic emission model (Guenther et al., 2006, Sakulyanontvittaya
204 et al., 2008) was used to estimate current and future biogenic VOC and soil NO_x
205 emissions based on the WRF meteorology with current and future estimates of land use
206 and land cover. For the current decade, the default MEGANv2.04 land cover and
207 emission factor data (Guenther et al., 2012) were used. For the future decade, cropland
208 distributions were estimated by combining three datasets: the IMAGE 2100 global

209 cropland extent dataset, (Zuidema et al., 1994), the SAGE maximum cultivable land
210 dataset (Ramankutty et al., 2002), and the MODIS-derived current cropland data (as used
211 in MEGANv2.04 and described in Guenther et al., 2006). The IMAGE 2100 dataset was
212 created from the output of a land cover model, which forms part of a sub-system of the
213 IMAGE 2.0 model of global climate change (Alcamo, 1994). The SAGE cultivable dataset
214 was created using a 1992 global cropland dataset (Ramankutty and Foley, 1998) modified
215 by characterizing limitations to crop growth based on both climatic and soil properties.
216 The future global cropland extent distribution was generated by analyzing predicted
217 changes in agriculture on a continent-by-continent basis (using the IMAGE data). These
218 changes were then applied to the MODIS based cropland map (used for present day
219 MEGAN simulations) using the SAGE maximum cultivable dataset as an upper limit to
220 cropland extent. The resulting land cover data has considerably lower cropland fraction
221 than the original IMAGE data, which likely overestimates future cropland area by not
222 considering whether a location is cultivable.

223 In addition to generating a future crop cover dataset to simulate potential biogenic
224 VOC emissions using MEGAN, future datasets representing several other MEGAN
225 driving variables were developed. These included geo-gridded potential future plant
226 functional type (PFT)-specific emission factor (EF) maps for isoprene and terpene
227 compounds, as well as future-extent maps of four non-crop PFTs: broadleaf trees,
228 needle-leaf trees, shrubs, and grasses. For regions outside of the US, the non-crop PFT
229 distributions were generated by reducing the current extent of each non-crop PFT map
230 by an amount that would appropriately offset the predicted cropland expansion for a given

231 continent. For the US, future non-crop PFT maps were generated using the Mapped
232 Atmosphere-Plant-Soil System (MAPSS) model output
233 (<http://www.fs.fed.us/pnw/corvallis/mdr/mapss/>; Neilson, 1995), based on three GCM
234 future scenarios. Present-day MAPSS physiognomic vegetation classes were associated
235 with current PFT fractional coverage estimates by dividing the US into sub-regions and
236 by averaging existing (MODIS-derived) geospatially explicit PFT data within each sub-
237 region as a function of MAPSS class. Sub-regions were created based on Ecological
238 Regions of North America (<http://www.epa.gov/wed/pages/ecoregions.htm>). After every
239 current MAPSS class had been assigned PFT-specific fractional coverage estimates,
240 future PFT cover was determined by re-classifying future distribution maps for the three
241 MAPSS datasets using the fractional PFT cover estimates for each MAPSS class (within
242 each ecological region), and averaging the three resultant future datasets into a single
243 estimate of future cover for each PFT.

244 For the eastern US, future isoprene and monoterpene PFT-specific EF maps were
245 constructed using changes in tree species composition predicted by the US [Department](#)
246 [of Agriculture](#) A-‘Climate Change Tree Atlas’ (CCTA, <http://nrs.fs.fed.us/atlas/tree/>). The
247 CCTA data [are](#) based on [ecosystem changes driven by](#) the average of three GCMs,
248 [which that](#) represented the most conservative emissions scenarios available.

249 Using existing speciated EF data (Guenther, 2013), we applied anticipated
250 changes in the average species composition of each PFT to generate species-weighted
251 PFT-specific EF maps on a state-by-state basis (the CCTA data is organized by state).

252 As data was lacking on predicted species-level changes for areas outside the eastern
253 US, we did not attempt to alter EF maps outside the eastern US.

254 **2.4 Anthropogenic Emissions**

255 For S-HEM domain CMAQ simulations, global emissions of ozone precursors from
256 anthropogenic, natural, and biomass burning sources were estimated for the period 1990-
257 2000 (applied to 1995-2004) using the POET emission inventory (Granier et al., 2005).
258 Non-US anthropogenic emissions (containing 15 sectors) were projected based on
259 national activity data and emission factors. Gridded maps (e.g. population maps) were
260 applied to spatially distribute the emissions within a country. The global emission
261 inventory for black and organic carbon (BC and OC respectively) was obtained from Bond
262 et al. (2004), which ~~uses~~ applies emission factors ~~on the basis~~ based of fuel type and
263 economic sectors alone. The Bond et al. (2004) inventory includes emissions from fossil
264 fuels, biofuels, open burning of biomass, and urban waste. Emissions are varied by
265 combustion practices, which consider ~~Considering~~ combinations of fuel, combustion type,
266 and emission controls, as well as their prevalence on a regional basis ~~covers the~~
267 ~~dependence of emissions on combustion practices.~~

268 Global emissions for the year 2000 from the POET, MEGAN, and Bond et al.
269 (2004) inventories were combined, and the 16 gas-phase POET and MEGAN species,
270 along with the OC and BC species were adapted to the SAPRC99 (Carter 1990, 2000)
271 chemical mechanism. Diurnal patterns were developed and applied to the gridded
272 emission inventories and processed using SMOKE. For the future decade hemispheric
273 domain simulations, current decade emissions were projected to the year 2050 based on

274 the IPCC A1B emission scenario. ~~After the emission inventories were combined and~~
275 ~~adapted to SAPRC99 and the diurnal patterns were applied, the differences percent~~
276 ~~change in emissions between the future and the current decade were~~ ~~estimated. To~~
277 ~~aid in understanding the effects of changes in global emissions upon the US, the percent~~
278 ~~change in emissions was summarized according to the regions and countries in the S-~~
279 ~~HEM domain that surround the CONUS domain (Figure 3).~~

280 ~~For the 36-km CONUS current decade CMAQ simulations,~~ US anthropogenic
281 emissions ~~for the 36-km CONUS current decade CMAQ simulations~~ were developed
282 using the 2002 National Emission Inventory. The Emission Scenario Projection (ESP)
283 methodology, version 1.0 (Loughlin et al., 2011), was applied to project future decade US
284 anthropogenic emissions. A primary component of ESP v1.0 is the MARKet Allocation
285 (MARKAL) energy system model (Loulou et al., 2004). MARKAL is an energy system
286 optimization model that characterizes scenarios of the evolution of an energy system over
287 time. In this context, the energy system extends from obtaining primary energy sources,
288 through their transformation to useful forms, to the variety of technologies (e.g., classes
289 of light-duty personal vehicles, heat pumps, or gas furnaces) that meet “end-use” energy
290 demands (e.g., projected vehicle miles traveled, space heating). Within ESP 1.0, ~~the~~
291 MARKAL is used to develop multiplicative factors that grow energy-related emissions
292 from a base year to a future year. Surrogates, such as projected population growth or
293 industrial growth, are used to develop non-energy-related growth factors. The resulting
294 factors were ~~used-applied~~ within SMOKE to develop a future decade inventory from the
295 2002 NEI inventory.

296 For the work presented here, the EPAUS9r06v1.3 database (Shay et al., 2006)
297 was used with MARKAL to develop growth factors for CO₂, NO_x, SO₂ and PM with
298 aerodynamic diameter smaller than 10 μm (PM_{10-2.5}). The PM₁₀ growth factors were also
299 applied to PM_{2.5}; and the CO₂ growth factors were used as a surrogate for energy system
300 CO, NH₃, VOC, HCl and chlorine. For mobile sources, NO_x growth factors were used for
301 CO, VOC, and NH₃. Non-combustion industrial emission growth factors were developed
302 from projections of economic growth. Growth factors for non-combustion emissions from
303 the residential and commercial sectors are linked to population growth. The resulting
304 energy and non-energy factors were then used within SMOKE to multiply emissions from
305 the 2002 National Emissions Inventory (NEI) to 2050.

306 EPAUS9r06v1.3 originally was calibrated to mimic the fuel use projections of the
307 U.S. Energy Information Administration's 2006 Annual Energy Outlook (AEO06; U.S.
308 DOE, 2008). Energy demands were adjusted to account for population growth consistent
309 with the A1B storyline. The results reflect business as usual assumptions about future
310 environmental and energy regulations as of 2006. Thus, while electric sector emissions
311 are capped to capture the effects of the Clean Air Interstate Rule (CAIR; US EPA, 2005),
312 the impacts of increases in natural gas availability, the -2007- economic downturn, and
313 the relatively new 54.5 Corporate Average Vehicle Efficiency (CAFÉ) standard (US CFR,
314 2011) are not reflected. More recent versions of the MARKAL database reflect these
315 factors with, expanded pollutant growth coverage, and refined emission factors (U.S.
316 EPA, 2013). The ESP v1.0, including the MARKAL database EPAUS9rv1.3, was selected
317 here to maintain compatibility with previous and ongoing activities.

318 ~~After SMOKE was used to develop a 2050 inventory,~~ The differences between the
319 base year and future-year US inventories were summarized at the pollutant and regional
320 level, ~~as are shown in~~ (Figure 4)3. Using the ESP v1.0 methodology, emissions of NO_x
321 and SO₂ are projected to decrease between 16% in the South and Southwest to 35% in
322 the Northeast and Northwest. On the other hand, emissions of pollutants that were not
323 captured endogenously ~~in by~~ MARKAL, such as carbon monoxide (CO), non-methane
324 volatile organic compounds (~~excluding methane; NMVOCs~~NMVOCs) and ammonia (NH₃)
325 are ~~projected~~ to increase in nearly all regions across the CONUS domain. The use
326 of surrogates for growth factors as described above means the projected changes in CO
327 and VOC emissions are likely too high. The largest increase (70%) of in emissions of CO
328 is projected in the Midwest; this is co-located ~~with a 70% increase combined~~ with an
329 increase of about 20% of NMVOC. The smallest increase of CO is projected for the South;
330 however, the same region was projected to increase NMVOC by about 12%. The largest
331 increase in PM_{2.5} emissions is projected in the Northwest (<20%) and tThe smallest
332 increase (3%) of PM_{2.5} is projected in the central region, which also has a projected 34%
333 increase in NMVOC.

334 2.5 Air Quality Simulations

335 The CMAQ model version 4.7.1 was employed to simulate the potential impact of
336 climate change on surface ozone and PM_{2.5} over the CONUS at 36 km horizontal grid
337 spacing and covering 18 vertical layers from the surface up to 100 mb. The model
338 configuration included the use of the SAPRC99 chemical mechanism and version 5 of the
339 aerosol module, with Secondary Organic Aerosol parameters of Carlton et al. (2010).

340 Methane concentration is fixed at 1.85 parts per million (ppm) for all CMAQ simulations.
341 Stratospheric intrusion (STE) was not included in the CMAQ simulations; ~~high~~ High STE
342 events are mostly relevant during the spring season, thus, lack of STE in our summer
343 simulations is not expected to have a significant effect in our results.

344

345 Using the framework components described above, a matrix of CMAQ simulations
346 that included changes in predicted meteorological conditions and potential emission
347 scenarios was constructed (Table 1). For each set of simulations shown in Table 1, five
348 representative summers were modeled. Simulation 0 represents the base case
349 simulation, where all model inputs are set to current decade conditions. Simulation 1 is
350 used to investigate the impact of climate change alone; ~~where~~ all model inputs are set to
351 current decade conditions except for meteorology (biogenic emissions are not allowed to
352 change with the future climate for this case). Simulation 2 is the same as Simulation 1,
353 except that biogenic emissions are allowed to change with the future climate, and in
354 Simulation 3, future land use is also incorporated into the biogenic emission estimates.
355 Simulation 4 is used to investigate the impact of future decade US anthropogenic
356 emissions, where all inputs are set to current decade levels except for US anthropogenic
357 emissions. The impact of future global emissions is investigated in Simulation 5. Finally,
358 ~~and~~ Simulation 6 represents the combined impacts of Simulations 1-5.

359 2.6 Evaluation of Model Performance

360 To aid in summarizing model results, the 36 km domain was divided geographically
361 into 7 regions (Figure 43, lower right). Since the WRF simulations used to drive CMAQ
362 are based on a climate realization rather than reanalysis data, a direct comparison
363 between the modeled output and observations cannot be made. Instead, the frequency
364 distributions of simulated and observed values are compared. For the simulated
365 meteorological fields, daily maximum temperature, and daily precipitation are compared
366 against a decade of summer observations (1995 to 2004) from the United States
367 Historical Climatological Network (US-HCN; http://cdiac.ornl.gov/ftp/ushcn_daily/; Karl et
368 al., 1990) in Figure 54. The model distributions of temperature and precipitation agree
369 reasonably well with the observations, and provide a good representation of the regional
370 variability of precipitation and temperature. Except for the Northwest and Southwest
371 regions, the observed mean and maximum temperatures are ~~slightly over predicted,~~ with
372 the largest overprediction in the Midwest, which is likely to result in higher emissions of
373 ozone and PM precursors from biogenic sources. ~~However, f~~ For all analyzed regions the
374 model successfully simulates the seasonal trend of summer temperatures, showing the
375 observed increase in mean temperature from June to July and subsequent decrease in
376 mean temperature from July to August (not shown).

377 The modeled daily maximum 8 hr ozone concentrations (DM8O) from the five
378 representative summers (Figure 65) from the current decade CMAQ simulations
379 (Simulation 0 in Table 1) were compared to the range of observations from the AIRNow
380 network (<http://airnow.gov/>). As seen in Figure 65, DM8O ~~tends to~~ be over-estimated in

381 regions where temperature maxima ~~is~~ are also over predicted, ~~such as the South,~~
382 ~~Midwest, Southeast and Northeast~~ most noticeably in the Midwest, the South, and the
383 Southeast but also in the Northeast. Except for the less populated Central region, DM8O
384 shows a bias that ranges between +10 ppb (+15%) and +25 ppb (+37%) across the
385 domain. This is consistent with previous climate downscaled results by Tagaris et al.
386 (2007), who found a bias of +15%, and with Avise et al. (2009), who found regional biases
387 as high as +39%. Despite the bias, results from the modeling framework presented here
388 have been shown to accurately represent the correlation between ozone and temperature
389 at rural Clean Air Status and Trends Network (CASTNET)-sites throughout the US (Avise
390 et al., 2012), suggesting that the bias in temperature is the main cause of the bias in
391 DM8O. This implies ~~and~~ that the chemical transport model is responding to the
392 meteorological driver of ozone production and thus can predict the impact of climate
393 change on DM8O.

394 Simulations for the current decade show a domain mean average DM8O of $66 \pm$
395 20 ppb (standard deviation between simulated DM8O for the five summers), while the
396 observed average at the AIRNow sites was 563 ± 189 ppb. The sSimulations successfully
397 captured the enhanced DM8O concentrations over the major urban areas and regions
398 with high biogenic sources (Figure 10231a, top). Interannual ~~v~~variability of the simulated
399 summertime DM8O concentrations ~~between summers~~ is on the order of 10% (not shown)
400 in highly populated areas and down to as little as 1% in less populated areas, with the
401 greatest variability found in the Northeast region.

402 Simulated concentrations of current decade PM_{2.5} (PM_{2.5} with no water content, unless
403 otherwise specified) show a five summer average of 12.056.9 ± 10.87 μg m⁻³, compared
404 to 14.3 ± 9.2 μg m⁻³ observed at the Speciation Trends Network (STN; US EPA, 2000).
405 ~~Simulated PM_{2.5} show the highest concentrations occurring inland of coastal regions and~~
406 ~~throughout the Northeast and Southeast (Figure 1421, top).~~

407 In general, the model slightly overestimates PM_{2.5} in the Midwest, the Southeast, and the
408 Northeast and significantly underestimates PM_{2.5} in the western half of the US (Figure 7).
409 Several factors contribute to the underestimation of PM_{2.5} in the western US, including a
410 lack of windblown dust and fire smoke emissions, and an underestimation of secondary
411 organic aerosol (SOA) formation (Carlton et al., 2010; Foley et al., 2010; Appel et al.,
412 2012; Luo et al., 2011). ~~In our study, when comparing to the STN data, we found an~~
413 ~~underestimation of all species, including SO₄²⁻ and total carbon (Organic Carbon +~~
414 ~~Elemental [Black] Carbon), except for the un-speciated PM_{2.5} species (also known as PM~~
415 ~~“other”). Nevertheless, when comparing the average fractional composition we found a~~
416 ~~slight overestimation of the SO₄²⁻ fraction for most regions (Figure 86, top panel). Most~~
417 ~~regions were also found to underestimate the NO₃⁻ and NH₄⁺ fractions. Low~~
418 ~~concentrations of NH₄⁺ relative to SO₄²⁻ result in a sulfate-rich system, where aerosols~~
419 ~~are dominated by aqueous phase HSO₄⁻ and SO₄²⁻ and have lower concentrations of~~
420 ~~(NH₄)₂SO₄ and NH₄NO₃ (Fountoukis and Nenes, 2007; Kim et al., 1993; Sienfield and~~
421 ~~Pandis, 2006). Further discussion of the response of the inorganic aerosol system to~~
422 ~~global changes is provided in Section 3.4.).~~ Another important factor that influenced the
423 underestimation of PM_{2.5} is the over-prediction of precipitation as shown in Figure 5

424 When compared to STN data (Figure 86, top panel), we found a large underestimation of
425 the fraction of organic carbon in all regions, while the unspecified fraction was over-
426 predicted. The unspecified fraction in CMAQ is composed of all the non-carbon atoms
427 associated with the OC fraction, unspecified direct PM_{2.5} emissions, and other trace
428 species (Foley et al., 2010). The underprediction in OC reflects the uncertainties in
429 precursor sources and the SOA formation mechanisms which have been previously
430 documented (e.g., Carlton et al., 2010; Foley et al., 2010).

431 Speciated PM_{2.5} model performance evaluation using mean fractional error (MFE) and
432 mean fractional bias (MFB) statistics for the major PM_{2.5} components as suggested by
433 Boylan and Russell (2006) was performed (Figure 86, middle and bottom panels). Overall,
434 the model has a large underestimation of organic carbon due to underestimation of SOA
435 as documented in previous studies (see compilation by Simon et al., 2012). To a less
436 degree the model also underestimates EC, SO₄²⁻, NO₃⁻, and NH₄⁺; this most likely is due
437 to overprediction of precipitation (Fig. 4b), but errors in other meteorological variables
438 and emissions also contribute to the underestimation. For the unspecified component, the
439 model meets the performance goal for 5 of the 7 regions. The majority of the speciated
440 components show MFE and MFB within the criteria threshold for most regions.
441 Furthermore, the model performance was within the criteria threshold these guidelines
442 for PM_{2.5} in four of the seven regions, and only in the Central region did the model not
443 meet these guidelines. Similarly, SO₄²⁻, NO₃⁻, NH₄⁺ and unspecified fractions meet the
444 benchmark thresholds for model performance in most regions. In terms of the unspecified
445 fraction, the better model performance in most regions is due to the heavy contribution to

446 ~~the total mass of the PM_{2.5}. For the SO₄²⁻-NO₃⁻-NH₄⁺ system, the values for the MFE and~~
447 ~~MFB indicate that the model performed sufficiently well in responding to the conditions~~
448 ~~that drive inorganic aerosol formation. These values increase the confidence about the~~
449 ~~response to global changes in the system. In the case of OC and EC, poor model~~
450 ~~performance was found, with concentrations largely underpredicted for all regions.~~

451 **3. Results and Discussion**

452 **3.1 Projected Changes in Meteorology**

453 For these types of climate change simulations, it is important to consider whether
454 the five selected summers represent the climatological conditions for the 1995-2004 and
455 2045-2054 periods. To address this, we compared the regional mean temperature and
456 total precipitation (Figure [978](#)) as well as maximum daily insolation and mean relative
457 humidity (not shown) for all ten summers versus the five selected summers. Based on the
458 two sample *t*-test, except for the Northwest region, we found no statistical difference in
459 the overall regional average conditions between the five and ten summer samples (*p*
460 >0.01). ~~The effect of selecting five summers instead of ten summers for the Northwest~~
461 ~~region is explained below.~~ For the purposes of this air quality assessment, this
462 comparison of the meteorological conditions for the five selected summers to the full ten
463 summer set of data suggest that the five summers provide a reasonable representation
464 of decadal summer meteorological conditions. While no statistical difference was found
465 between the five and ten summer samples, some distinct features should need to be
466 highlighted: 1) For the current decade, except for the Southeast, the former chosen set
467 of five summers on average represents an average warmer current decade is slightly

468 warmer than the average of the ten summers sample; 2) The five summers chosen
469 for current and future decades. Five-year summer led to a projection of cooling in the
470 Northwest average represent a decrease in future temperature in the Northwest region.
471 The effects of the higher average temperature as result of the five summer sample, and
472 the projected decrease in future temperature in the Northwest region are explained
473 discussed below.

474 Similar to the 30 year meteorological variability assessment carried out by
475 Andersson and Engardt (2010), the differences between current and future summer
476 meteorological conditions, based on the five representative periods, were found to be
477 significant at the 99% confidence level for all regions except for the Northwest. This further
478 supports the use of five representative summers as the basis for the air quality
479 assessment of current and future conditions.

480 Projected changes in selected meteorological parameters are shown in Figure
481 9108. Except for some minor cooling along the Pacific coast, the resulted of selecting five
482 versus ten summers, mean summer temperature across the continental US is projected
483 to increase between 0.5°C and 4°C (Figure 9108a). This increase falls within the lower
484 bound of the warming predicted by the ensemble of 20 GCM's under the A1B emission
485 scenario described by Christensen et al., (2007), but differs in the regional variability due
486 to the higher resolution of our simulations. When compared to similar studies of equal
487 resolution using a GCM (e.g. Goddard Institute for Space Studies (GISS) GCM II') driven
488 by the A1B IPCC emission scenario and downscaled with MM5 to 36-km resolution, our
489 simulated temperatures show higher temperature differences between future and current

490 decades (Leung and Gustafson, 2005; Tagaris et al., 2007). ~~Furthermore,~~ Tagaris et al.
491 (2007) and Leung and Gustafson (2005) predicted an average increase of between 1 and
492 3 °C for most of ~~the domain~~ CONUS, and temperature reductions in the border states of
493 the Central and South regions. Nevertheless, despite the differences in physical
494 parameterizations contained in the GCMs and the driving IPCC emission scenarios that
495 were used, similar temperature differences (2 to 4 °C) between our study and previous
496 investigations were simulated for the Northeast and Southeast regions (Leung and
497 Gustafson, 2005; Tagaris et al., 2007; Avise et al., 2009).

498 Projected increases in solar radiation reaching the ground vary by region. A
499 decrease in solar radiation in the Northwest that extends to the northern boundaries of
500 the Central regions is simulated. Small changes in the Southwest, South and Midwest are
501 also predicted, with the largest increase experienced in the Northeast and Southeast
502 regions (Figure ~~910~~ 8b). Similar results for the Northeast regions are reported ~~for~~ by
503 previous investigations (Leung and Gustafson, 2005; Tagaris et al., 2007, and Avise et
504 al., 2009); ~~h~~ However, these same investigations had higher reductions in solar radiation
505 at the border states between the Central and South regions.

506 Projected changes in precipitation across the US also vary depending on the
507 region. With the exception of the Northwest and the northern boundary of the Central
508 region, summertime precipitation is projected to decrease between -10% and -80%. The
509 largest decrease is projected in the Southwest region. Our results show greater
510 precipitation reductions than those presented in Christensen et al., (2007), who predicted
511 projected between a -5 to -15% decreases in the South and Southwest regions. Also,

512 previous investigations agreed with our ~~predicted-projected~~ mean precipitation reductions
513 across the domain (Figure ~~9108~~c). In the Northwest, the modeled increase in precipitation
514 is ~~also~~ consistent with Leung and Gustafson (2005), who projected an increase in
515 precipitation throughout the Northwest region. In contrast, the Southeast and Northeast
516 regions show disparities in the magnitude and the sign of the change in precipitation.
517 While our simulations ~~predict-show~~ a reduction in precipitation between -10 to -20%, the
518 ensemble of 20 GCM's in Christensen et al., (2007) ~~predicted-resulted in~~ an increase
519 between 5 to 10% across ~~these same~~ regions. The disparities~~y~~ may be a result of the
520 differences in resolution and parameterization schemes between our study and those
521 used for the 20 GCM's.

522 Changes in relative humidity are shown in Figure ~~9108~~d. Relative humidity is
523 ~~predicted-shown~~ to decrease in most of the domain except for the regions where
524 decreases in solar radiation were projected. The greater decrease in relative humidity
525 occurs in the Southwest and Central regions of the domain, and the largest increase is
526 observed in the Northwest region.

527 **3.2 Changes in Biogenic Emissions**

528 Average summertime isoprene emissions over five summers of simulation for each
529 decade are shown in Figure 10a. ~~As expected, i~~isoprene emissions occur at relatively
530 high rates (>50 metric tons/day) in the eastern US and at much lower rates in the western
531 US (<10 metric tons/day). Under future climate conditions and current land use, isoprene
532 and monoterpene emissions are projected to increase in all regions except for the
533 Northwest (Figs. 4 and 10b); this follows the spatial pattern of projected temperature

534 changes (Fig. 9a).— The most noticeable increases occur in the Northeast and Southeast
535 regions. The model projects bigger percentage increase in monoterpenes than isoprene
536 across the domain; however, total isoprene emission is an order of magnitude higher and
537 thus dominates the changes in total BVOC. The increase in total BVOC ranges between
538 17% and 45%. The only region that is projected to have reduced total BVOC emissions
539 is the Northwest, where, ~~despite the increase in monoterpenes,~~ the model simulates a
540 7% reduction in isoprene emissions (Figure ~~43~~)- that in absolute amount is greater than
541 the 20% increase in ~~simulated~~ monoterpene emissions~~is simulated~~. The reduction in
542 isoprene emissions in the Northwest is a result of the decrease in temperatures in areas
543 the coastal area where the higher isoprene emissions are encountered (Figure ~~9108a~~).

544 ~~Furthermore, despite projects having the bigger percentage biggest increases~~
545 ~~in monoterpenes than isoprene across the US domain, s are the latter still drives the~~
546 ~~absolute change in the Central and South regions, the larger increase in isoprene for the~~
547 ~~Midwest, followed by the Northeast, Southeast, South, Central and Southwest regions,~~
548 ~~drives the increase in total BVOC in emissions of BVOC. The increase in BVOC ranges~~
549 ~~between 17% and 45%. Previous investigations (Liao et al., 2006, Nolte et al., 2008) show~~
550 ~~the greatest increase in BVOC emissions in the Southeast region (10-50%). Similarly,~~
551 ~~Leung and Gustafson (2005) predicted the greatest increase in BVOC in the Southeast,~~
552 ~~but did not show any significant changes in the Northwest region.~~

553 ~~Average summertime isoprene emissions over five summers of simulation for each~~
554 ~~decade are shown in Figure 1019a. As expected, isoprene emissions occur at relatively~~
555 ~~high rates (>50 metric tons/day) in the eastern US and at much lower rates in the western~~

556 US (<10 metric tons/day). ~~When the emissions are projected to future climate conditions~~
557 ~~with current land use distributions, isoprene emissions are projected to increase across~~
558 ~~the domain (average increase of about 30%; Figure 1019b) with the most noticeable~~
559 ~~increases occurring in the Northeast and Southeast regions. However, w~~When future
560 climate is combined with future land use to project biogenic emissions, ~~there are still~~
561 ~~increases in the eastern US, but the spatial extent of~~ isoprene emission ~~the increase is~~
562 reduced, reflecting the expansion of low isoprene-emitting croplands into regions of high
563 isoprene-emitting deciduous forests. In this case, the domain-average increase was
564 approximately 12% of current decade emissions, compared with a 25% increase when
565 changes in land use are not included (Figure 1120a). Thus, future expansion of cropland
566 and subsequent reduction of broadleaf forested lands are projected to lessen the overall
567 increase in US isoprene emissions that result from a warmer climate. When the future
568 decade meteorology is combined with future land use, an increase of over 100% of
569 current decade monoterpene emissions is predicted (Figure 11b). The growth is most
570 noticeable in the Central, South and Midwest regions. Also, an overall increase between
571 25% and 50% for the western and eastern regions is ~~predicted~~simulated. This limited
572 increase is primarily driven by the projected changes in land use predicted for those
573 regions.

574 ~~Future monoterpene emission estimates increase because of higher~~ temperatures
575 ~~across the domain.~~ Since the version of MEGAN used in this work does not include the
576 suppression of isoprene emissions due to elevated concentrations of CO₂ (Rosenstiel et
577 al., 2003; Heald et al., 2009), the future estimates in this study are likely to be an upper

578 bound on isoprene emissions, and it is likely that future isoprene emissions will be lower
579 than predicted by this work. Monoterpene emissions from US landscapes are not
580 expected to be suppressed by increasing CO₂ and so are not impacted by omitting this
581 process.

582 ~~When the future decade meteorology is combined with future land use (Figure~~
583 ~~1120b), an increase of over 100% of current decade monoterpene emissions is predicted.~~
584 ~~The growth is most noticeable in the Central, South and Midwest regions. Also, an overall~~
585 ~~increase between 25% and 50% for the Western and Eastern regions is predicted. This~~
586 ~~limited increase is primarily driven by the projected changes in land use predicted for~~
587 ~~those regions.~~

588 **3.3 Effects of Global Changes upon Ozone Concentrations**

589 Results for how the various global changes affect summertime DM8O are
590 summarized in Table 232 and Figure 1231. Simulations for the future decade (Simulation
591 6) show a domain average of 48 ± 11 ppb with higher DM8O ~~across the domain~~ in the
592 Northwest, Central and South regions than the current decade simulation (Simulation 0)
593 ~~with a domain average of 51 ± 10 ppb~~. In general, increases in DM8O are due to growing
594 global anthropogenic emissions and climate change, while decreasing US emissions
595 reduce DM8O. Changes in biogenic emissions as a result of a changing climate and land
596 use have less of an influence on DM8O ~~than intercontinental transport~~ increase of global
597 anthropogenic emissions; the influence can be either positive or negative depending on
598 ~~the region. These various factors~~ that influence future DMO3 are discussed in the
599 following sections.

600 3.3.1 Contributions from Changes in Global and Regional US Anthropogenic 601 Emissions

602 The effects of increased long-range transport of global emissions ~~from Asia and~~
603 ~~Mexico~~ are shown in Figure 1234f. The changes in chemical boundary conditions (the
604 difference between Simulations 0 and 5 ~~in Table 1~~) ~~increase~~ DM8O between ~~242~~ to ~~656~~
605 ppb across the CONUS domain. The general west-to-east ~~and south-to-north~~ gradient of
606 the change in DM8O reflects intercontinental and regional transport of ozone and its
607 precursors from the west and from Mexico at the south. The greatest impact ~~is~~
608 ~~predicted~~ occurs in the South (6ppb) (~~6 ppb~~) and Southwest (5 ppb) (~~4 ppb~~) regions. These
609 results show a smaller influence in DM8O from the intercontinental transport than the
610 simulations presented in ~~are consistent with~~ Avise et al., (2009), who ~~show~~ reported
611 increases between 3 and 6 ppb of DM8O across the domain, with the greatest increase
612 in the Southwest and South regions. The higher effect from intercontinental transport
613 presented in Avise et al., (2009) is due to higher ~~larger~~ increases in ~~NOx emissions of~~
614 NOx from global anthropogenic sources under the SRES A2 emission scenario. The
615 effects of future global emissions and intercontinental transport of ozone precursors in
616 the continental US have also been investigated by Hogrefe et al. (2004), who predicted
617 an increase of 5 ppb in the Northeast region under the SRES A2 ~~IPCC~~ emission scenario.

618 Changes in regional US emissions of ozone precursors (difference between
619 Simulations 0 and 4) reduce DM8O concentrations between 2 and 15 ppb ~~across the~~
620 ~~domain~~ in most of eastern US, most of western US, and Texas. Projected increases in
621 ozone in urban areas near the coasts are mainly due to the limited representation of the
622 heavy duty, shipping and rail sectors on the ESPv1.0 (Loughlin et al.,— 2012) by which

623 [local steady or increase in emissions of NO_x and VOCs in ports are the main cause of](#)
624 [increase in ozone in those urban areas. Regionally, larger reductions are observed in](#)
625 the Southeast (-3%) and Southwest (-3.5%) regions with a reduction of 5 ppb and the
626 Northeast (-2.3%) and South (-0.9%) regions with a reduction of 3– [ppb \(Figure 12e,](#)
627 [Table 2\)](#). Similar results are shown in Nolte et al., (2008) and Tagaris et al., (2007) despite
628 a difference in the magnitude of projected emissions reductions. Tagaris et al., (2007)
629 simulated similar ozone reductions (about 9%), with a higher nationwide reduction of 51%
630 in NO_x emissions and a slight increase (about 2%) in VOC emissions from ~~A1B~~
631 projections based on the Clean Air Interstate Rule (CAIR) emission inventory. Nolte et
632 al., (2008) showed a decrease in ozone across the domain (-12 to -16 ppb) as a result of
633 projected reductions of 45% for NO_x and 21% for VOC emissions from the NEI 2002,
634 following the [SRES_A1B-IPCC](#) emission scenario. In contrast, our future simulations
635 included a [3821%](#) reduction in NO_x emissions and a slight increase (about 2%) in VOC
636 emissions. Avise et al., (2009) predicted an average contribution of +3 ppb across the
637 domain as a result of projecting the NEI 1999 (NEI-1999) with the Economic Growth
638 Analysis System (EGAS) and the [SRES_A2-IPCC](#) emission scenario; increasing
639 emissions by 5% for NO_x and 50% for VOCs in the future. ~~The smaller~~ [lower reduction in](#)
640 [ozone concentrations between the future and the current decade in comparison to Nolte](#)
641 [et al., \(2008\) is likely to be a consequence of the increase in VOC and CO emissions from](#)
642 [the resulted of the current version of the MARKAL databasebusiness-as-usual scenario](#)
643 [of MARKAL, which, as explained in section 2.4, uses CO₂ as a diverse surrogates for](#)
644 [growth factors for CO and VOC \(Loughlin et al. 2011\).](#)

645 3.3.2 Contributions from Changes in Meteorological Fields

646 Figure 1234b shows the difference between simulations that include changes in
647 meteorological conditions (without the effect of biogenic emissions or land use) and the
648 current decade base case (Simulations 0 and 1). The local greater reductions in DM8O
649 concentrations in the Northwest and Southwest regions resulted from an increase in cloud
650 cover and lower solar radiation reaching the ground, and which causes resulting in a
651 reduction in photochemistry due to lower solar radiation reaching the ground (Figure
652 9108b), similar to the results of Jacob and Winner, 2009. Nevertheless, For other regions,
653 increases in DM8O concentrations were projected (+5 ppb) because of increases in
654 temperature had a greater impact on the ozone chemistry and solar insolation; this is
655 particularly evident in the Central, Midwest, Northeast and Southeast regions eastern half
656 of the US.

657 3.3.3 Contributions from Changes in Biogenic Emissions and Future Land Use

658 When biogenic emissions are allowed to change with the future meteorology, an
659 average increase of DM8O with respect to the current decade base case simulations is
660 predicted (Simulations 0 and 32). Increases of as much as 7 ppb in DM8O concentrations
661 are mainly predicted in areas with substantial biogenic sources (Figure 1234c). Similar
662 results are shown by Leung and Gustafson-Nolte et al. (20085) and Tagaris et al. (2007),
663 ; both predicted an increase of DM8O above 5 ppb in the east coast. Simulated
664 reductions between 2 to 4 ppb of DM8O in the coastal areas of the western regions are
665 probably due to cooler temperatures and reduced solar insolation (Figure 9a, b) increased
666 cloud cover. Minor changes in DM8O concentrations are shown over the Southwest and
667 Northwest regions. This is in agreement with Avise et al. (2009) and Nolte et al., Leung

668 ~~and Gustafson (20085)~~ who predicted reductions in DM8O concentrations from 1 to 4 ppb
669 in the western regions, while Tagaris et al. (2007) also predicted similar reductions in
670 ozone in the Central and Midwest regions. The disparities between this investigation and
671 Avise et al. (2009) are reasonable due to the different climate realizations used (A2 vs.
672 A1B; Storyline in scenario A2 consider higher emissions of CO₂ by 2050 than the scenario
673 A1B). However, ~~the~~ the difference in geographical features of ~~ozone-DM8O~~ changes with
674 ~~Leung and Gustafson~~ Nolte et al. (20085) and Tagaris et al. (2007) suggests that the
675 source of disparities resides in ~~both: the simulated regional meteorological fields resulted~~
676 ~~of the different global climate models, modeling systems, as discussed by Weaver et al.~~
677 ~~(2009); regional climate models both the climate realization and~~ the methods used to
678 estimate emissions from biogenic sources. We used the ECHAM5 global climate model
679 results while both Nolte et al. (2008) and Tagaris et al. (2007) used results from the GISS
680 global climate model. For regional climate simulations, we used WRF; while both Nolte
681 et al. (2008) and Tagaris et al. (2007) used MM5 while we used WRF here. In contrast
682 with Nolte et al. (2008) and Tagaris et al. (2007) who use the BEIS/BELD3 (Hanna et al.,
683 2005; <http://www.epa.gov/chief/emch/biogenic/>) tool to compute biogenic emissions, this
684 investigation estimates the biogenic emissions with MEGAN v2.04, which MEGAN v2.04,
685 which generally predicts higher isoprene ~~emission~~emissions than BEIS (Hogrefe et al.,
686 2011; Sakulyanontvittaya et al., 2012). is known to produce Hogrefe et al. (2011) showed
687 that for the Northeast using MEGAN leads to higher DM8O in the Northeast by upwards
688 of 7 ppb for under the scenario of 2005 anthropogenic emissions; however, underfor a
689 scenario by which anthropogenic NO_x emissions were reduced by ~60%, difference in

690 DM8O was generally 3 ppb because of due to greater sensitivity to NO_x emissions when
691 MEGAN was used. higher concentrations of ozone than BEIS (Hogrefe et al., 2014)

692 When the results from Simulation 2 (Fig. 12c) are compared to the climate-only
693 simulations (Simulation 1, Fig. 12b), our results suggest that changes in the
694 meteorological fields are the main driver of DM8O enhancement in Simulations 2 and 3
695 (Fig. 12c and d) across the domain. Even though BVOC emissions are higher in
696 Simulation 2 relative to Simulation 1, Simulation 2 resulted in 2 to 4 ppb lower DM8O in
697 the Southeast. This decrease is associated with a decrease reduction in NO_x
698 concentrations (Fig. 14a). ~~This decrease in NO_x concentrations leads~~
699 ~~to an increase in the VOC concentrations to NO_x ratio relative to the climate-only~~
700 ~~(Simulation 1). The decrease between the Simulation 2 and Simulation 1 in our~~
701 ~~simulated DM8O suggests that the effect of sequestration of ozone precursors NO_x by the~~
702 ~~biogenic VOCs as organic nitrates (RNO₃) is predominant over the effect of recycling of~~
703 ~~NO_x organic isoprene nitrates (RNO₃) considered in SAPRC-99, which lumps all non-PAN~~
704 ~~organic nitrates as one compound that has a NO_x recycling efficiency of about 30%.~~ A
705 similar effect was reported by The simulated is reduction in ozone is consistent with the
706 results of Xie, et al. (20122013), who simulated reported an increases in NO_x and of 2
707 ppb of ozone in the Southeast when sequestration by isoprene nitrates was reduced in
708 the relative to the chemical mechanism base SAPRC-07T mechanism that has the same
709 RNO₃ treatment as SAPRC-99. Evidence of the predominant effect of sequestration over
710 the recycling of organic nitrates NO_x in the Southeastern US is shown seen in Figure
711 145, where which shows a an increase in RNO₃ and reduction in the NO_x concentrations

(Figure 145a) and the consequent decrease in the NO_x to RNO₃ ratio (RNO₃; Figure 145b) in most of the eastern US in the for sSimulation 2 relative to sSimulation 1 is observed. Furthermore, when land use changes are included along with biogenic emissions (Simulation 3; Figure 14d), the increase in BVOC emissions is projected to be less while NO_x emission is projected to increase in areas where natural vegetation is converted to cropland. This combination leads to ratio is reduced and less depletion in higher DM8O is simulated in Simulation 3 than, thus, higher concentrations of DM8O than the Simulation 2 (Simulation 3; Figure 1234d) are also observed. This lower VOC to NO_x ratio is due to the increase in soil NO and the reduction of BVOC emissions associated with the land use change from natural vegetation to cropland.

3.3.4 Contributions from Combined Global Change to Future Changes in DM8O Concentrations

When the combined global changes are considered (Simulation 6), DM8O is projected to increase in all regions, except with local reductions along the western coastlines in the Northwest, Central and South nearly all regions except along the western and eastern coastlines and inland areas of those regions. Increases of DM8O between 14 to 3712 ppb in the NorthwestSouth, Southwest and Central and MidwesNortheast regions are shown along with a local reductions-increase of 1 to 634 ppb in parts of the South, Midwest and Centralwest and Northwest-Midwest regions (Figure 1234g). The increase in DM8O is mostly due to an increase in global emissions of ozone precursors from the semi-hemispheric domain, which contributes to an increase of 2-6 ppb under current climate conditions (Figure 1234f). The other contributing factors to increasing DM8O are a combination of ~~changed~~ meteorological changesy (Figure

735 1231b) and higher BVOC emissions (with current and future land use; Figure 1231c,d).
736 Reductions in DM8O in the urban areas resulted generally from reductions in ozone
737 precursors from regional anthropogenic sources (Figure 1231e). However, in the western
738 regions, lower DM8O are the result of a combination of favorable meteorological
739 conditions (e.g. reduction in temperature and solar radiation reaching the ground) and
740 reductions in regional ozone precursors.

741 3.4 Effects of Global Changes upon PM_{2.5} Concentrations

742 Results for how the various global changes affect PM_{2.5} concentrations and
743 composition are summarized in Tables 34-56 and Figure 134. Overall, projected increase
744 in US anthropogenic emissions have the largest impact on PM_{2.5}, with leading to an
745 increase in concentrations in all regions.— Changes in global emissions do not have a
746 significant impact on PM_{2.5} concentrations, while changes in the climate and biogenic
747 emissions can lead to both increases and decreases in PM_{2.5} depending on the region.

748 3.4.1 Contribution to PM_{2.5} Concentrations from Changes in Global and Regional 749 Anthropogenic Emissions

750 The results from this study are similar to those reported by~~Similar results are~~
751 shown in Avise et al. (2009), who predicted a change in PM_{2.5} of less than 1 µg m⁻³ as a
752 result of changes in future chemical boundary conditions. In our simulation, the highest
753 increase in PM_{2.5} concentrations is found in the South region (< 1%). This increase in the
754 South region is indicative of the effects of increased emissions from Mexico (Figure 13f).
755 ~~Due to the relatively short atmospheric lifetime of PM, the effects from long-range~~
756 ~~transport and increasing global emissions on US PM_{2.5} concentrations are relatively small~~
757 ~~in comparison to the current decade PM_{2.5} concentrations~~PM_{2.5} concentrations increase

758 ~~by 8-10% in the South, Southwest, Central, and Northwest regions, with a south to north~~
759 ~~gradient indicative of the effects of increased emissions from Mexico (Figure 12f). Similar~~
760 ~~results are shown in Avise et al. (2009), who predicted a change of less than $1 \mu\text{g m}^{-3}$ as~~
761 ~~a result of changes in future chemical boundary conditions. However, w~~When ~~the~~
762 chemical composition is analyzed, Table 3~~simulations~~ shows an increase in aerosol
763 nitrate (NO_3^-) in nearly all regions except for the South ~~(Table 33)~~; these increases are
764 less than $0.1 \mu\text{g m}^{-3}$, as a result of increased global NH_3 emissions. In contrast, similar to
765 the results of Avise et al. (2009) ~~predicted no change in NO_3^- for the same regions.~~
766 Furthermore, in our simulation, increases between 3% and 8% in SO_4^{2-} and NH_4^+ in the
767 Southwest, Central and South regions are mostly a result of increase in emissions of SO_2
768 and NH_3 from Mexico. Similarly, Avise et al. (2009) showed higher future concentrations
769 (by 7% to 25%) of SO_4^{2-} for the same regions resulting from higher global SO_2 emissions.
770 In our simulations, cChanges in global anthropogenic emissions cause reductions in SOA
771 in the Southwest, Central, South, regions and ~~an~~ increases in the Northwest, Midwest,
772 Southeast and Northeast Regions (Table 44); ~~However,~~ the simulated changes in SOA
773 are very small ~~($< 1.3\%$ and $< 0.05 \mu\text{g m}^{-3}$)~~ and the variation ~~is probably~~ may be due to
774 small differences in modeled OH radical concentrations.

775 In the US, reductions in regional SO_2 and NO_x emissions from regulatory
776 curtailment on electricity generation are offset by the projected increase ~~and further~~
777 ~~speciation of primary~~ in emissions of $\text{PM}_{2.5}$ and NH_3 from other sources; thus, resulting in
778 an overall increase in $\text{PM}_{2.5}$ concentrations between 1 and $4 \mu\text{g m}^{-3}$ across ~~the~~
779 ~~nation~~ CONUS. Similarly, Avise et al. (2009) predicted an average increase of $3 \mu\text{g m}^{-3}$

780 across the domain but as a result of increasing NO_x and SO₂ from anthropogenic sources.
781 The greatest increase, between 2 to 4 µg m⁻³, is found in the urban areas across the
782 Northwest, Northeast, Midwest and Southeast region (Figure 132e) as a result of increase
783 in primary emissions of PM_{2.5}. Similarly, Trail et al., (2015) find an increase in PM_{2.5}
784 concentrations between 1 and 2 µg m⁻³ as a result of an scenario that consider changes
785 in fuel use. In contrast, Tagaris et al. (2007),⁷ predicted a decrease of 23% as a result of
786 decreasing emissions. Increase in SOA concentrations ~~is also~~ resulted from higher
787 emissions of NMVOC and an increase in primary organic aerosol from anthropogenic
788 sources in the US.⁷ (Table 4).

789 In terms of the inorganic PM_{2.5} components, reductions in SO₂ and NO_x emissions
790 in the US are offset by higher emissions of primary SO₄²⁻ sulfate and nitrate and ammonia
791 NO₃⁻ and NH₃, leading to an increase in both sulfate and ammonium aerosol in the form
792 of ammonium sulfate and ammonium bisulfate. When eCompared to Tagaris et al. (2007),
793 our investigation shows no reduction in SO₄²⁻ sulfate concentrations as a result of smaller
794 reduction in SO₂ emissions from anthropogenic sources. Furthermore, similar to
795 Shimadera et al.,⁷ (2013) the increase in NO₃ nitrate concentrations in the form of
796 ammonium nitrate is highly dependent on the increase in NH₃ emissions and insensitive
797 less sensitive to changes in emissions of NO_x.

798 **3.4.2 Contribution to PM_{2.5} concentrations from global climate change alone**

799 Despite the effect of precipitation on PM loading, as it washes out the precursors
800 and the existing PM from the atmosphere (Seinfeld and Pandis, 2006), the effect of
801 climate change alone (with no change to biogenic emissions) on total PM_{2.5}

802 concentrations over land is a change of less than $1 \mu\text{g m}^{-3}$ (Figure 123b). However, the
803 change in $\text{PM}_{2.5}$ composition due to climate change is highly variable and depends on
804 changes in temperature, relative humidity and precipitation. Increases in reaction rate
805 constants of SO_2 and higher oxidant concentrations from increased temperature and solar
806 insolation lead to an increase in aerosol sulfate formed ~~and thus are correlated with~~
807 ~~changes in SO_4^{2-} concentrations~~ (Dawson et al., 2007). ~~—~~ Relative humidity and
808 temperature affect the thermodynamic equilibrium of $\text{SO}_4^{2-}\text{-NH}_4^+\text{-NO}_3^-$, especially the
809 partitioning of HNO_3 between the gas and particulate phases.

810 For all regions, sulfate concentrations are predicted to increase by 3-10%. Except
811 for the Northwest regions, this change in concentrations is consistent with decreased
812 precipitation, which reduces wet deposition, and increases in temperature and solar
813 insolation, which increase radical production rates and increases the oxidation of SO_2 to
814 produce aerosol sulfate. The same increase in temperature leads to nitrate being more
815 volatile and thus decreases aerosol nitrate concentrations in regions where sulfate
816 concentrations are predicted to increase. For the same regions where SO_4^{2-} sulfate is
817 projected to increase, higher concentrations of radicals also lead to higher oxidation of
818 VOC, thus increasing SOA concentrations in the same regions.

819 While increasing precipitation is generally associated with decreasing $\text{PM}_{2.5}$,
820 results here for the Northwest region showed an increase in $\text{PM}_{2.5}$ despite an increase in
821 precipitation (Figure 132b). This suggests the effects of slightly colder temperature and
822 higher relative humidity in this region, leading to an enhanced formation of
823 $(\text{NH}_4)\text{NO}_3$ ammonium nitrate (Table 3). Furthermore, the increase in relative humidity in

824 the Northwest and the coastal areas of the Southwest regions leads to the increase in
825 production of sulfate aerosol via aqueous reaction (Luo et al., 2011). Higher
826 concentrations of ammonium nitrate(NH_4NO_3) ~~and, in addition to~~ higher concentrations
827 of SOA (Table 44) indicate increased aerosol formation, ~~appear to~~ dominate over the
828 effect of precipitation.

829 **3.4.3 Contribution to $\text{PM}_{2.5}$ concentrations from changes in biogenic emissions** 830 **and future land use**

831 Simulations that consider projected climate change as well as the associated
832 change in biogenic emissions (Simulation 2) show an increase in $\text{PM}_{2.5}$ between 0.5 and
833 $3 \mu\text{g m}^{-3}$; ~~These~~ these changes are mainly reflected in areas with high biogenic sources
834 (Figure 132c). When the effects of future land use are considered (Simulation 3), an
835 increase in the geographical extent of $\text{PM}_{2.5}$ is observed in comparison to the climate and
836 biogenic emissions case, and higher increases (up to $6 \mu\text{g m}^{-3}$) of $\text{PM}_{2.5}$ are predicted in
837 parts of the South, Southwest~~Southwest~~Southeast, Midwest and Northeast regions (Figure 123d).
838 This is primarily due to the increase in emissions of sesquiterpenes (not shown) and
839 monoterpenes (Figure 110b), leading to more SOA being formed.

840 In terms of the inorganic components of $\text{PM}_{2.5}$, the effect of climate change is still
841 the predominant factor for the change in SO_4^{2-} sulfate concentrations for the Central,
842 South, Midwest and Southeast regions (Table 3). The ~~lessen~~ smaller increase or absolute
843 reduction in SO_4^{2-} sulfate in comparison to the climate-only case is due to the competition
844 between BVOC and SO_2 for the availability of OH, which is an oxidant for both.
845 Additionally, a ~~lessen~~ smaller decrease in NO_3^- in most of the domain and increase in the
846 Northwest is predicted due to changes in the availability of OH as a result of the changes

847 in emissions of BVOC and soil NO. The increase in availability of OH and increase in soil
848 NO emissions lead to higher formation of aAmmonium nNitrate in Ssimulations 2 and 3
849 than in Ssimulation 1.

850 SOA concentrations are predicted to increase as a result of higher emissions of
851 BVOC across the domain (Table 4). Furthermore, when climate change and biogenic
852 emissions are combined with future land use, concentrations of SOA are predicted to
853 increase up to 121% in the Central region and up to 188% in the Southeast due to
854 increased biogenic monoterpene and sesquiterpene emissions (not shown).

855 **3.4.4 Changes in Precursors and PM_{2.5} Concentrations from the Combined Global** 856 **Changes**

857 Table 5 shows the summary of changes to PM_{2.5} as a result for all Simulations of
858 the individual and combined global changes presented above. The differences in PM_{2.5}
859 between the future decade and current decade base case are greater in the eastern half
860 of the US compared to the western half. In the eastern half of the US, the largest increases
861 in PM_{2.5} occur in the Southeast. Our results show that the 2 to 10 $\mu\text{g m}^{-3}$ increase in PM_{2.5}
862 in the Southeast region is dominated by higher concentrations of SOA due to increased
863 biogenic emissions as a result of climate change (Figure 123c), changes in land use
864 (Figure 132d; Table 4) and increase in anthropogenic emissions (Figure 132e). Table 5
865 indicates that the combination of climate change, biogenic emissions and land use, and
866 increase in anthropogenic emissions increases the concentrations of PM_{2.5} between 27
867 and 78 % depending on the region.

868 4. Conclusions

869 We have investigated the individual and combined contributions of factors that
870 impact US air quality by dynamically downscaling future climate projections using the
871 WRF model and using the regional chemical transport model CMAQ version 4.7.1.
872 Decreases in future US anthropogenic ozone precursor emissions are the only
873 consistently ~~positive~~-beneficial influence that improves the ~~ozone concentrations~~air
874 quality in the US and updated assumptions to generate scenarios of future US
875 anthropogenic emissions may ~~improve such influences~~show even more positive influence.
876 However that positive influence is offset by 1) ~~changes in long range transport and~~
877 increasing global emissions and changes in long range transport, which have a negative
878 impact on air quality across the domain; 2) climate changes (namely, increased
879 temperatures and solar radiation), which increase ozone concentrations in the Central,
880 South, Midwest, Northeast and Southeast regions of the domain; and 3) increases in US
881 BVOC emissions, which also increase ozone concentrations in regions with high biogenic
882 emissions such as the South, Midwest, Northeast and Southeast.

883 In the case of the overall concentrations of PM_{2.5}, our results indicate that the
884 effects of increasing biogenic emissions in addition to increase primary PM from
885 anthropogenic sources have an overall negative impact on air quality by increasing PM_{2.5}
886 concentrations between 27 to 78%. In terms of the PM_{2.5} composition, we show a
887 regionally dependent mixture of inorganic aerosols and SOA. For the case of the
888 Southeast, our findings indicate that increases in BVOC may result in higher
889 concentrations of PM_{2.5}. This effect extends to the Midwest and Northeast regions due to

890 changes in land use. Furthermore, meteorological changes or regulatory curtailment, as
891 incorporated in these simulations do not offset the increasing concentrations of primary
892 PM and BVOC. In addition, synergistic effects of changes in meteorological parameters
893 and changes in emission may shift the composition of the inorganic fraction of PM_{2.5} in
894 the ~~western~~ US. The synergistic effects of increase of ~~SO₄~~ sulfate and SOA in the urban
895 areas of the coastal regions of the Northwest and Southwest leads to an increase in PM_{2.5}
896 in those regions, off-setting decreases due to increased precipitation and temperature,
897 and reduced primary anthropogenic emissions of SO₂ and NO_x.

898 In conclusion, the results of this study suggest that the efforts to improve air quality
899 through low emission technologies and public policy directed to the electricity generation
900 sector may not have a major effect if future emissions ~~of primary PM~~ from other sectors
901 ~~are~~ are allowed to increase. In addition, higher global anthropogenic emissions, a warmer
902 future world and the effects of these changes on emissions from biogenic sources may
903 increasingly undermine all regulatory efforts. Consequently, additional measures may be
904 necessary to improve air quality in the US.

905 Much of the modeling components used for this research carry different levels of
906 complexity and have reached diverse stages of development, thus, subsequent research
907 intended to assess the effect of climate change and future regional emissions upon air
908 quality would benefit from newer versions of the emission inventories (e.g. 2011); updated
909 assumptions on the US emission projections (e.g. New versions of MARKAL with the use
910 of the ESP 2.0 methodology); newer versions of MEGAN that take into account the
911 isoprene emission suppression due to CO₂ concentrations and more realistic estimates

912 of land use change; and the inclusion of emissions from wildfires and the consequent
913 effect upon air quality.

914

915 **Acknowledgments**

916 This work was supported by the U.S. Environmental Protection Agency Science
917 To Achieve Results Grants RD 83336901-0 and 838309621-0. This paper has been
918 cleared by the EPA's administrative review process and approved for publication. The
919 views expressed in this paper are those of the authors and do not necessarily reflect the
920 views or policies of the US Environmental Protection Agency.

References

Alcamo, J: IMAGE 2.0 : integrated modeling of global climate change, Kluwer Academic, Dordrecht., 1994.

Andersson, C. and Engardt, M.: European ozone in a future climate: Importance of changes in dry deposition and isoprene emissions, *J. Geophys. R.*,115(D2), D02303, D02303, 2010.

Ambrose, J.L., Reidmiller, D.R., and Jaffe, D.A.: Causes of high O₃ in the lower free troposphere over the Pacific Northwest as observed at the Mt. Bachelor Observatory. *Atmos. Environ.*, 45, 5302–5315, 2011.

Appel, K. W., Chemel, C., Roselle, S. J., Francis, X. V., Hu, R. M., Sokhi, R. S., Rao, S. T. and Galmarini, S.: Examination of the Community Multiscale Air Quality (CMAQ) model performance over the North American and European domains, *Atmos. Environ.*, 53, 142-155, 2012.

Avise, J., Abraham, R. G., Chung, S. H., Chen, J., Lamb, B., Salathé, E. P., Zhang, Y., Nolte, C. G., Loughlin, D. H. and Guenther, A.: Evaluating the effects of climate change on summertime ozone using a relative response factor approach for policymakers, *J. Air Waste. Manage.*, 62(9), 1061–1074, 2012.

Avise, J., Chen, J., Lamb, B., Wiedinmyer, C., Guenther, A., Salathé, E. and Mass, C.: Attribution of projected changes in summertime US ozone and PM_{2.5} concentrations to global changes, *Atmos. Chem. Phys.*, 9, 1111–1124, 2009.

Aw, J. and Kleeman, M. J.: Evaluating the first-order effect of intraannual temperature variability on urban air pollution, *J. Geophys. Res.*, 108(D12), 4365, 2003.

Bond, T. C., Streets, D. G., Yarber, K. F., Nelson, S. M., Woo, J. H. and Klimont, Z.: A technology-based global inventory of black and organic carbon emissions from combustion, *J. Geophys. Res.*, 109(D14), D14203, 2004.

Boylan, J. W. and Russell, A. G.: PM and light extinction model performance metrics, goals, and criteria for three-dimensional air quality models, *Atmos. Environ.*, 40(26), 4946–4959, 2006.

Byun, D. and Schere, K. L.: Review of the governing equations, computational algorithms, and other components of the Models-3 Community Multiscale Air Quality (CMAQ) modeling system, *Appl. Mech. Rev.*, 59(1/6), 51, 2006.

Carlton, A. G., Bhave, P. V., Napelenok, S. L., Edney, E. O., Sarwar, G., Pinder, R. W., Pouliot, G. A. and Houyoux, M.: Model representation of secondary organic aerosol in CMAQv4. 7, *Environ. Sci. Technol.*, 44(22), 8553–8560, 2010.

Carter, W. P. L. :A detailed mechanism for the gas-phase atmospheric reactions of organic compounds, *Atmos. Environ., Part A, General Topics* 24, 481e518, 1990.

Carter, W.P.L.: Documentation of the SAPRC-99 Chemical Mechanism for VOC Reactivity Assessment. Report to the California Air Resources Board. Available at: <http://cert.ucr.edu/wcarter/absts.htm#saprc99>; <http://www.cert.ucr.edu/wcarter/reactdat.htm>, 2000.

Chen, J., Avise, J., Guenther, A., Wiedinmyer, C., Salathe, E., Jackson, R. B. and Lamb, B.: Future land use and land cover influences on regional biogenic emissions and air quality in the United States, *Atmos. Environ.*, 43(36), 5771 – 5780, doi:10.1016/j.atmosenv.2009.08.015, 2009a.

Chen, J., Avise, J., Lamb, B., Salathé, E., Mass, C., Guenther, A., Wiedinmyer, C., Lamarque, J. F., O'Neill, S. and McKenzie, D.: The effects of global changes upon regional ozone pollution in the United States, *Atmos. Chem. Phys.*, 9, 1125–1141, 2009b.

Christensen, J.H., B. Hewitson, A. Busuioc, A. Chen, X. Gao, I. Held, R. Jones, R.K. Kolli, W.-T. Kwon, R. Laprise, V. Magaña Rueda, L. Mearns, C.G. Menéndez, J. Räisänen, A. Rinke, A. Sarr and P. Whetton, 2007: Regional Climate Projections. In: *Climate Change.: The Physical Science Basis. Contribution of Working Group I to the Fourth Assessment Report of the Intergovernmental Panel on Climate Change* [Solomon, S., D. Qin, M. Manning, Z. Chen, M. Marquis, K.B. Averyt, M. Tignor and H.L. Miller (eds.)]. Cambridge University Press, Cambridge, United Kingdom and New York, NY, USA, 2007.

[Cooper, O. R., Gao, R.-S., Tarasick, D., Leblanc, T. and Sweeney, C.: Long-term ozone trends at rural ozone monitoring sites across the United States, 1990-2010, *J. Geophys. Res.*, 117, doi:10.1029/2012JD018261, 2012.](#)

[Cooper, O. R., Parrish, D. D., Stohl, A., Trainer, M., Nedelec, P., Thouret, V., Cammas, J. P., Oltmans, S. J., Johnson, B. J., Tarasick, D., Leblanc, T., McDermid, I. S., Jaffe, D., Gao, R., Stith, J., Ryerson, T., Aikin, K., Campos, T., Weinheimer, A. and Avery, M. A.: Increasing springtime ozone mixing ratios in the free troposphere over western North America, *NATURE*, 463\(7279\), 344–348, doi:10.1038/nature08708, 2010.](#)

Dadvand, P., Parker, J., Bell, M.L., Bonzini, M., Brauer, M., Darrow, L., Gehring, U., Glinianaia, S.V., Gouveia, N., Ha, E.-H., et al.: Maternal Exposure to Particulate Air Pollution and Term Birth Weight: A Multi-Country Evaluation of Effect and Heterogeneity. *Environ. Health Persp.*, 2012.

[Day, M. C. and Pandis, S. N.: Effects of a changing climate on summertime fine particulate matter levels in the eastern U.S.: AIR QUALITY IN A CHANGING CLIMATE, *J. Geophys. Res.*, 120\(11\), 5706–5720, doi:10.1002/2014JD022889, 2015.](#)

Dawson, J. P., Adams, P. J. and Pandis, S. N.: Sensitivity of PM_{2.5} to climate in the Eastern US: a modeling case study, *Atmos. Chem. Phys.*, 7, 4295–4309, 2007.

[Dawson, J. P., Racherla, P. N., Lynn, B. H., Adams, P. J. and Pandis, S. N.: Impacts of climate change on regional and urban air quality in the eastern United States: Role of meteorology, *Journal of Geophysical Research: Atmospheres*, 114\(D5\), D05308, doi:10.1029/2008JD009849, 2009.](#)

Dawson, J. P., Bloomer, B. J., Winner, D. A. and Weaver, C. P.: Understanding the meteorological drivers of U.S. particulate matter concentrations in a changing climate, *Bull. Amer. Meteor. Soc.*, doi:10.1175/BAMS-D-12-00181.1, 2013.

Dulière, V., Zhang, Y. and Salathé Jr., E. P.: Changes in twentieth-century extreme temperature and precipitation over the western United States based on observations and regional climate model simulations. *J. Climate*, 26, 8556-8575, doi:10.1175/JCLI-D-12-00818.1, 2013.

Dulière, V., Zhang, Y. and Salathé Jr., E. P.: Extreme Precipitation and Temperature over the U.S. Pacific Northwest: A Comparison between Observations, Reanalysis Data, and Regional Models, *J. Climate*, 24(7), 1950–1964, doi:10.1175/2010JCLI3224.1, 2011.

Fiore, A. M., West, J. J., Horowitz, L. W., Naik, V. and Schwarzkopf, M. D.: Characterizing the tropospheric ozone response to methane emission controls and the benefits to climate and air quality, *J. Geophys. Res.*, 113, D08307, doi:10.1029/2007JD009162, 2008.

Foley, K. M., Roselle, S. J., Appel, K. W., Bhave, P. V., Pleim, J. E., Otte, T. L., Mathur, R., Sarwar, G., Young, J. O., Gilliam, R. C., Nolte, C. G., et al.: Incremental testing of the Community Multiscale Air Quality (CMAQ) modeling system version 4.7, *Geoscientific Model Development*, 3(1), 205–226, doi:10.5194/gmd-3-205-2010, 2010.

Fountoukis, C. and Nenes, A.: ISORROPIA II: a computationally efficient thermodynamic equilibrium model for K⁺–Ca²⁺–Mg²⁺–NH₃, *Atmos. Chem. Phys.*, 7, 4639–4659, 2007.

Forkel, R. and Knoche, R.: Regional climate change and its impact on photooxidant concentrations in southern Germany: Simulations with a coupled regional climate-chemistry model, *J. Geophys. Res.*, 111(D12), doi:10.1029/2005JD006748, 2006.

Giorgi, F. and Meleux, F.: Modelling the regional effects of climate change on air quality, *C. R. Geosci.*, 339(11–12), 721 – 733, doi:http://dx.doi.org/10.1016/j.crte.2007.08.006, 2007.

Granier, C., J.F. Lamarque, A. Mieville, J.F. Muller, J. Olivier, J. Orlando, J. Peters, G. Petron, G. Tyndall, S. Wallens.: POET a database of surface emissions of ozone precursors, available on internet at <http://www.aero.jussieu.fr/projet/ACCENT/POET.php>, (accessed on 2005).

Grell, G. A., Dudhia, J., and Stauffer, D. R.: A Description of the Fifth-Generation Penn State/NCAR Mesoscale Model (MM5), National Center for Atmospheric Research, Boulder, CO, USA, NCAR/TN-398+STR., 122 pp, 1994.

Guenther, A., T. Karl, P. Harley, C. Wiedinmyer, P. I. Palmer, C. Geron.: Estimates of global terrestrial isoprene emissions using MEGAN (Model of Emissions of Gases and Aerosols from Nature), *Atmos. Chem. Phys.*, 6, 3181-3210, 2006.

Guenther, A. B., X. Jiang, C. L. Heald, T. Sakulyanontvittaya, T. Duhl, L. K. Emmons, and X. Wang: The Model of Emissions of Gases and Aerosols from Nature version 2.1 (MEGAN2.1): an extended and updated framework for modeling biogenic emissions, *Geoscience Model Development*, 5(6), 1471-1492. 2012.

Guenther, A.: Biological and Chemical Diversity of Biogenic Volatile Organic Emissions into the Atmosphere, *ISRN Atmospheric Sciences*, doi: 10.1155/2013/786290. 2013.

[Hanna, S. R., Russell, A. G., Wilkinson, J. G., Vukovich, J. and Hansen, D. A.: Monte Carlo estimation of uncertainties in BEIS3 emission outputs and their effects on uncertainties in chemical transport model predictions, *J. Geophys. Res.*, 110\(D1\), doi:10.1029/2004JD004986, 2005.](#)

Heald, C. L., M. J. Wilkinson, R. K. Monson, C. A. Alo, G. Wang, and A. Guenther.: Response of isoprene emission to ambient CO₂ changes and implications for global budgets, *Global Change Biol.*, 15, 1127-1140., 2009.

[Hogrefe, C., Isukapalli, S. S., Tang, X., Georgopoulos, P. G., He, S., Zalewsky, E. E., Hao, W., Ku, J.-Y., Key, T. and Sistla, G.: Impact of biogenic emission uncertainties on the simulated response of ozone and fine particulate matter to anthropogenic emission reductions, *J Air Waste Manag Assoc*, 61\(1\), 92–108, 2011.](#)

Hogrefe, C., Lynn, B., Civerolo, K., Ku, J. Y., Rosenthal, J., Rosenzweig, C., Goldberg, R., Gaffin, S., Knowlton, K. and Kinney, P. L.: Simulating changes in regional air pollution over the eastern United States due to changes in global and regional climate and emissions, *J. Geophys. Res.*, 109(D22), D22301, 2004.

Horowitz, L. W.: Past, present, and future concentrations of tropospheric ozone and aerosols: Methodology, ozone evaluation, and sensitivity to aerosol wet removal, *J. Geophys. Res.*, 111(D22), D22211, 2006.

Huang, H.-C., Liang, X.-Z., Kunkel, K. E., Caughey, M. and Williams, A.: Seasonal Simulation of Tropospheric Ozone over the Midwestern and Northeastern United States: An Application of a Coupled Regional Climate and Air Quality Modeling System, *J. Appl. Meteor. Climatol.*, 46(7), 945–960, doi:10.1175/JAM2521.1, 2007.

Huang, H.-C., Lin, J., Tao, Z., Choi, H., Patten, K., Kunkel, K., Xu, M., Zhu, J., Liang, X.-Z., Williams, A., Caughey, M., Wuebbles, D. J. and Wang, J.: Impacts of long-range

transport of global pollutants and precursor gases on U.S. air quality under future climatic conditions, *J. Geophys. Res.*, 113(D19), doi:10.1029/2007JD009469, 2008.

Intergovernmental Panel on Climate Change and Intergovernmental Panel on Climate Change: *Climate change 2007: the physical science basis: contribution of Working Group I to the Fourth Assessment Report of the Intergovernmental Panel on Climate Change*, Cambridge University Press, Cambridge ; New York., 2007.

Jacob, D. J. and Winner, D. A.: Effect of climate change on air quality, *Atmos. Environ.*, 43(1), 51 – 63, doi:10.1016/j.atmosenv.2008.09.051, 2009.

Karl, T. R., J. C.N. Williams, F. T. Quinlan, and T.A. Boden.: *United States Historical Climatology Network (HCN) Serial Temperature and Precipitation Data*. Vol. 3404, Environmental Science Division Publication, Carbon Dioxide Information and Analysis Center, Oak Ridge National Laboratory, 389 pp, 1990

Kelly, J., Makar, P. A., and Plummer, D. A.: Projections of mid-century summer air-quality for North America: effects of changes in climate and precursor emissions, *Atmos. Chem. Phys.*, 12, 5367–5390, doi:10.5194/acp-12-5367-2012, 2012.

Kim, Y.P., Seinfeld, J.H., and Saxena, P.: Atmospheric gas-aerosol equilibrium I. Thermodynamic model. *Aerosol Sci. Tech.*, 19, 157–181, 1993.

Kunkel, K. E., Huang, H. C., Liang, X. Z., Lin, J. T., Wuebbles, D., Tao, Z., Williams, A., Caughey, M., Zhu, J. and Hayhoe, K.: Sensitivity of future ozone concentrations in the northeast USA to regional climate change, *Mitigation Adapt. Strategies Global Change*, 13(5), 597–606, 2007.

Langner, J., Bergstrom, R. and Foltescu, V.: Impact of climate change on surface ozone and deposition of sulphur and nitrogen in Europe, *Atmos. Environ.*, 39(6), 1129–1141, doi:10.1016/j.atmosenv.2004.09.082, 2005.

Lelieveld, J., and Dentener, F.: What controls tropospheric ozone? *J. Geophys. Res.*, 105, 3531-3551, 2009

Leung, L. R. and Gustafson, W. I.: Potential regional climate change and implications to US air quality, *Geophys. Res. Lett.*, 32, L16711, 2005.

Leung L.R., Kuo Y.H., Tribbia J.: Research needs and directions of regional climate modeling using WRF and CCSM. *B Am Meteorol Soc.*, 87,1747–1751, 2006

Liao, H., Chen, W. T. and Seinfeld, J. H.: Role of climate change in global predictions of future tropospheric ozone and aerosols, *J. Geophys. Res.*, 111(D12), D12304, 2006.

Liang, X.-Z., Pan, J., Zhu, J., Kunkel, K. E., Wang, J. X. L. and Dai, A.: Regional climate model downscaling of the U.S. summer climate and future change, *J. Geophys. Res.*, 111(D10), doi:10.1029/2005JD006685, 2006.

Lin, J.-T., Patten, K.O., Hayhoe, K., Liang, X-Z., Wuebbles, D.J.: Effects of future climate and biogenic emissions changes on surface ozone over the United States and China, *J. Appl. Meteor. Climatol*, 47, 1888-1909, 2008.

[Lin, M., Fiore, A. M., Horowitz, L. W., Cooper, O. R., Naik, V., Holloway, J., Johnson, B. J., Middlebrook, A. M., Oltmans, S. J., Pollack, I. B., Ryerson, T. B., Warner, J. X., Wiedinmyer, C., Wilson, J. and Wyman, B.: Transport of Asian ozone pollution into surface air over the western United States in spring: *J Geophys Res.*, 117\(D21\), doi:10.1029/2011JD016961, 2012.](#)

Loughlin, D.H., Benjey, W.G. and Nolte, C.G.: ESP 1.0: Methodology for exploring emission impacts of future scenarios in the United States, *Geoscientific Model Development*, 4, 287-297, 2011.

Loulou R, G. Goldstein and K. Noble. 2004. Documentation for the MARKAL family of models. Energy Technology Systems Analysis Programme: Paris, France. <http://www.etsap.org/tools.htm>. (Accessed September 15, 2011)

Luo, C., Wang, Y., Mueller, S. and Knipping, E.: Diagnosis of an underestimation of summertime sulfate using the Community Multiscale Air Quality model, *Atmos. Environ.*, 45(29), 5119–5130, 2011.

Meleux, F., Solmon, F., Giorgi, F.: Increase in summer European ozone amounts due to climate, *Atmos. Environ.*, 7577–7587, 2007.

Nakicenovic, N., et al.: IPCC Special Report on Emissions Scenarios. Cambridge, UK: Cambridge University Press, 2000.

Neilson, R. P.: A Model for Predicting Continental-Scale Vegetation Distribution and Water Balance. *Ecol. Appl.*, 5(2), 362-385, 1995

Nolte, C. G., Gilliland, A. B., Hogrefe, C. and Mickley, L. J.: Linking global to regional models to assess future climate impacts on surface ozone levels in the United States, *J. Geophys. Res.*, 113, D14307, 2008.

Otte, T. L. and Pleim, J. E.: The Meteorology-Chemistry Interface Processor (MCIP) for the CMAQ modeling system: updates through MCIPv3.4.1, *Geoscientific Model Development*, 3(1), 243–256, doi:10.5194/gmd-3-243-2010, 2010.

[Racherla, P. N. and Adams, P. J.: Sensitivity of global tropospheric ozone and fine particulate matter concentrations to climate change, *J. Geophys. Res.*, 111\(D24\), D24103, doi:10.1029/2005JD006939, 2006.](#)

Racherla, P. N. and Adams, P. J.: The response of surface ozone to climate change over the Eastern United States, *Atmos. Chem. Phys.*, 8, 871–885, 2008.

Raes, F., Liao, H., Chen, W. T. and Seinfeld, J. H.: Atmospheric chemistry-climate feedbacks, *J. Geophys. Res.*, 115(D12), D12121, 2010.

Ramankutty, N., Foley, J.A., Norman, J., and K. McSweeney.: The global distribution of cultivable lands: Current patterns and sensitivity to possible climate change, *Global Ecol. Biogeogr.*, 11, 377-392, 2002.

Ramankutty, N., and J.A. Foley.: Characterizing patterns of global land use: An analysis of global croplands data, *Global Biogeochem. Cy.*, 12(4), 667-685, 1998.

Ravishankara, A. R., Dawson, J. P. and Winner, D. A.: New Directions: Adapting air quality management to climate change: A must for planning, *Atmos. Environ.*, 50(0), 387 – 389, doi:<http://dx.doi.org/10.1016/j.atmosenv.2011.12.048>, 2012.

Roeckner E., Bengtsson L., Feichter J., Lelieveld J., Rodhe H.: Transient climate change simulations with a coupled atmosphere-ocean GCM including the tropospheric sulfur cycle, *J. Climate*, (12)3004-3032, 1999.

Roeckner E, Bauml G, Bonaventura L, Brokopf R, Esch M, Giorgetta M, Hagemann S, Kirchner I, Kornbleuh L, Manzini E, Rhodin A, Schelse U, Schulzweida U, Tomkins A.: The atmospheric general circulation model ECHAM5, Part I: model description, Max-Planck Institute of Meteorology Report No. 349, 2003.

Rosenstiel, T. N., M. J. Potosnak, K. L. Griffin, R. Fall, and R. K. Monson.: Increased CO₂ uncouples growth from isoprene emission in an agriforest ecosystem. *Nature*, 421 (6920), 256– 259, 2003.

[Sakulyanontvittaya, T., G. Yarwood, A. Guenther: Improved biogenic emission inventories across the West – Final Report. ENVIRON International Corporation, Novato, California. March 19. \(http://www.wrapair2.org/pdf/WGA_BiogEmisInv_FinalReport_March20_2012.pdf\)](http://www.wrapair2.org/pdf/WGA_BiogEmisInv_FinalReport_March20_2012.pdf)

Sakulyanontvittaya, T., T. Duhl, C. Wiedinmyer, D. Helmig, S. Matsunaga, M. Potosnak, J. Milford, and A. Guenther.: Monoterpene and sesquiterpene emission estimates for the United States, *Environ. Sci. Tech.*, 42(5), 1623-1629. 2008

Salathé, E., Leung, L., Qian, Y. and Zhang, Y.: Regional climate model projections for the State of Washington, *Climatic Change*, 102(1), 51–75, 2010.

Seinfeld, J. H., & Pandis, S. N.: *Atmospheric Chemistry and Physics: From air pollution to climate change* (2nd Edition ed.), New Jersey: John Wiley and Sons, Inc, 2006.

Shay, C.L., Yeh, S., Decarolis, J., Loughlin, D.H., Gage, C.L. and Wright, E.: EPA U.S. National MARKAL Database: Database Documentation. U.S. Environmental Protection Agency, Washington, DC, EPA/600/R-06/057, 2006.

[Shimadera, H., Hayami, H., Chatani, S., Morino, Y., Mori, Y., Morikawa, T., Yamaji, K. and Ohara, T.: Sensitivity analyses of factors influencing CMAQ performance for fine particulate nitrate, J. Air Waste. Manage, 64\(4\), 374–387, doi:10.1080/10962247.2013.778919, 2014.](#)

Steiner, A. L., S. Tonse, R. C. Cohen, A. H. Goldstein, and R. A. Harley.: Influence of future climate and emissions on regional air quality in California, J. Geophys. Res., 111, D18303, 2006

Tagaris, E., Manomaiphiboon, K., Liao, K.-J., Leung, L. R., Woo, J.-H., He, S., Amar, P. and Russell, A. G.: Impacts of global climate change and emissions on regional ozone and fine particulate matter concentrations over the United States, J. Geophys. Res., 112(D14), doi:10.1029/2006JD008262, 2007.

Tao, Z., Williams, A., Huang, H. C., Caughey, M. and Liang, X. Z.: Sensitivity of US surface ozone to future emissions and climate changes, Geophys. Res. Lett., 34(8), L08811, 2007.

[Trail, M. A., Tsimpidi, A. P., Liu, P., Tsigaridis, K., Hu, Y., Rudokas, J. R., Miller, P. J., Nenes, A. and Russell, A. G.: Impacts of Potential CO₂-Reduction Policies on Air Quality in the United States, Environmental Science & Technology, 49\(8\), 5133–5141, doi:10.1021/acs.est.5b00473, 2015.](#)

Unger, N. Shindal, D.T., Koch, D.M., Amann, M., Cofala, J., Streets, D.G.: Influences of man-made emissions and climate changes in tropospheric ozone, methane and sulfate at 2030 from a broad range of possible futures. J. Geophys. Res., 111, D12313, 2006.

United States Code of Federal Regulations (US CFR). 2017-2025 model year light-duty vehicle GHG and 904 CAFE standards: supplemental notice of intent. United States 905. Federal Register 76(153) 2011.

U.S. Department of Energy. Energy Information Administration (US EIA). Annual Energy Outlook 2008 with Projections to 2030, DOE/EIA-0383(2008), U.S. Department of Energy: Washington, D.C., 2008.

U.S. Environmental Protection Agency (US EPA). Clean Air Interstate Rule emissions inventory technical support document, US Environmental Protection Agency, Office of Air Quality Planning and Standards, Research Triangle Park, NC, available at: <http://www.epa.gov/cair/pdfs/finaltech01.pdf>(last access: March 2011), 2005

US. Environmental Protection Agency (EPA): National Ambient Air Quality Standards for Ozone, Proposed Rule, Federal Register, 75(11), 2938-3052, 2010.

US Environmental Protection Agency (EPA): Quality assurance guidance document-Final quality assurance project plan: PM_{2.5} speciation trends network field sampling (EPA-454/R-01-001). US environmental protection agency, Office of air quality planning and standards, Research triangle park, NC, 2000.

U.S. Environmental Protection Agency (US EPA). Office of Research and Development. EPA U.S. Nine Region MARKAL Database: Database Documentation. NTIS number forthcoming. Research Triangle Park, N.C., 2013.

Washington, W. M., Weatherly, J. W., Meehl, G. A., Semtner, A. J., Bettge, T.W., Craig, A. P., Strand, W. G., Arblaster, J., Wayland, V. B., James, R., and Zhang, Y.: Parallel Climate Model (PCM) control and transient simulations. *Climate Dyn.*, 16(10–11), 755–774, 2000.

Weaver, C. P., Cooter, E., Gilliam, R., Gilliland, A., Grambsch, A., Grano, D., Hemming, B., Hunt, S. W., Nolte, C., Winner, D. A., Liang, X.-Z., et al.: A Preliminary Synthesis of Modeled Climate Change Impacts on U.S. Regional Ozone Concentrations, *Bull. Amer. Meteor. Soc.*, 90(12), 1843–1863, doi:10.1175/2009BAMS2568.1, 2009.

Wuebbles, D.J., Lei, H., and Lin, J.: Intercontinental transport of aerosols and photochemical oxidants from Asia and its consequences. *Environ. Pollut.*, 150, 65–84, 2007.

World Health Organization (WHO): Air quality guidelines for particulate matter, ozone, nitrogen dioxide and sulfur dioxide: Summary of risk assessment. 2005

World Meteorological Organization (WMO): Global Atmosphere Watch: WMO/iGAC Impacts of Megacities on Air Pollution and Climate, 2012

Wu, S., Mickley, L.J., Leibensperger, E.M., Jacob, D.J., Rind, D., Streets, D.G.: Effects of 2000-2050 global change on ozone air quality in the United States. *J. Geophys. Res.*, 113, D06302., 2008a

Wu, S., Mickley, L.J., Jacob, D.J., Rind, D., Streets, D.G.: Effects of 2000-2050 changes in climate and emissions on global tropospheric ozone and the policy-relevant background ozone in the United States. *J. Geophys. Res.*, 113, D18312., 2008b

Xie, Y., Paulot, F., Carter, W. P. L., Nolte, C. G., Luecken, D. J., Hutzell, W. T., Wennberg, P. O., Cohen, R. C. and Pinder, R. W.: Understanding the impact of recent advances in isoprene photooxidation on simulations of regional air quality, *Atmos. Chem. Phys.*, 13(16), 8439–8455, doi:10.5194/acp-13-8439-2013, 2013.

Zhang, Y., Qian, Y., Dulière, V., Salathé Jr., E. P., and Leung, L. R.: ENSO anomalies over the Western United States: present and future patterns in regional climate simulations, *Climatic Change*, 110(1-2), 315–346, doi:10.1007/s10584-011-0088-7, 2012.

Zhang, Y., Olsen, S. C., and Dubey, M. K.: WRF/Chem simulated springtime impact of rising Asian emissions on air quality over the U.S.. *Atmos. Environ.*, 44, 2799-2812, 2010.

Zhang, Y., Dulière, V., and Salathé Jr., E. P.: Evaluation of WRF and HadRM mesoscale climate simulations over the United States Pacific Northwest. *J. Climate*, 22, 5511-5526, 2009.

Zhang, L., Jacob, D.J., Downey, N.V., Wood, D.A., Blewitt, D., Carouge, C.C., Van Donkelaar, A., Jones, D., Murray, L.T., and Wang, Y.: Improved estimate of the policy-relevant background ozone in the United States using the GEOS-Chem global model with 1/2 times 2/3 horizontal resolution over North America. *Atmos. Environ.*, 45, 6769–6776, doi:10.1016/j.atmosenv.2011.07.054, 2011

Zuidema, G., Born, G. J., Alcamo, J. and Kreileman, G. J. J.: Simulating changes in global land cover as affected by economic and climatic factors, *Water Air and Soil Pollution*, 76(1-2), 163–198, doi:10.1007/BF00478339, 1994.

Table 1. List of simulations to assess the effect of global climate changes upon air quality in the United States

	Climate	Biogenic Emissions		Anthropogenic Emissions	
		Climate	Land Use	US	Global
0	Current	Current	Current	Current	Current
1	Future	Current	Current	Current	Current
2	Future	Future	Current	Current	Current
3	Future	Future	Future	Current	Current
4	Current	Current	Current	Future	Current
5	Current	Current	Current	Current	Future
6	Future	Future	Future	Future	Future

Table 2. Percent change in DM8O between each future scenario and the current decade base case.

Region	Climate (1)	BVOC (2)	BVOC Future Land Use (3)	US emissions (4)	Boundary Conditions (5)	Combined (6)
DM8O						
Northwest	0.4	-1.0	-0.8	-0.6	8.1	4.5
Southwest	2.0	0.4	0.0	-3.5	9.1	4.2
Central	5.6	4.5	4.9	-0.1	8.9	12.3
South	6.2	4.3	6.1	-0.9	9.6	13.0
Midwest	7.6	7.2	8.5	0.0	2.6	10.0
Northeast	8.2	6.6	7.6	-2.3	1.4	5.3
Southeast	8.6	6.1	7.7	-3.0	3.3	6.1

Table 334. Percent change in the aerosol NH_4^+ , SO_4^{2-} and NO_3^- between each future scenario and the current decade base case. The corresponding simulation number for each sensitivity simulation is shown in parenthesis

Region	Climate (1)	Climate & BVOC (2)	Climate, BVOC, Land Use (3)	US Anthropogenic Emissions (4)	Boundary Conditions (5)	Combined (6)
NH_4^+						
Northwest	15.7	-0.6	-0.9	12.8	-0.2	12.2
Southwest	3.4	-8.8	-7.9	4.2	8.2	4.8
Central	12.5	2.1	2.7	6.9	3.3	14.8
South	9.1	4.3	5.8	7.5	4.8	22.9
Midwest	5.1	0.6	3.3	12.2	0.4	18.1
Northeast	1.8	-5.0	-4.2	17.5	-0.3	12.7
Southeast	10.0	5.0	4.8	12.4	0.5	21.3
SO_4^{2-}						
Northwest	10.0	-5.4	-5.3	6.3	0.9	1.6
Southwest	5.4	-4.6	-4.0	0.7	6.2	2.8
Central	10.9	1.5	2.0	3.4	3.2	10.1
South	7.3	3.7	4.7	1.5	4.8	14.5
Midwest	7.2	1.8	4.1	2.7	0.4	10.9
Northeast	3.5	-4.0	-3.2	3.2	-0.2	2.3
Southeast	8.8	3.5	2.9	1.9	0.8	9.3
NO_3^-						
Northwest	-0.3	2.3	0.9	20.3	6.4	27.4
Southwest	-10.1	-8.0	-7.3	11.8	8.2	12.7
Central	-34.4	-17.1	-12.0	87.6	2.6	68.4
South	-7.0	-18.7	-11.5	38.5	-2.0	17.0
Midwest	-38.4	-31.1	-23.6	96.6	2.6	56.4
Northeast	-43.9	-43.2	-42.1	74.0	2.0	4.8
Southeast	-29.4	-28.7	-28.7	54.6	7.5	19.6

Table 4-45 Percent change of ~~secondary organic aerosol~~SOA and ~~primary organic carbon~~ between each future scenario and the current decade base case. The corresponding simulation number for each sensitivity simulation is shown in parenthesis

Region	Climate (1)	Climate & BVOC (2)	Climate BVOC & Land Use (3)	US Anthropogenic Emissions (4)	Boundary Conditions (5)	Combined (6)
SOA						
Northwest	11.6	17.5	40.7	17.4	1.3	61.1
Southwest	2.2	20.3	31.9	10.2	-0.2	41.0
Central	16.2	43.9	118.6	7.1	-0.2	126.4
South	4.7	57.0	113.2	7.4	-0.4	121.3
Midwest	16.0	48.6	121.2	7.9	0.1	131.0
Northeast	17.9	59.5	108.8	9.8	0.2	119.1
Southeast	14.2	73.2	135.1	8.1	0.3	143.5

Table 5 Percent change of PM_{2.5} between each future scenario and the current decade base case. The corresponding simulation number is shown in parenthesis

Region	Climate (1)	BVOC (2)	BVOC Future Land Use (3)	US emissions (4)	Boundary Conditions (5)	Combined (6)
PM2.5						
Northwest	7.0	2.1	7.3	43.2	-0.8	51.7
Southwest	3.3	3.3	7.1	20.7	0.7	27.8
Central	10.5	12.6	31.0	14.5	0.0	46.5
South	5.4	21.3	40.5	17.6	1.0	60.8
Midwest	7.8	15.2	37.6	22.4	0.1	61.2
Northeast	7.8	16.0	30.4	28.5	0.0	58.3
Southeast	10.6	29.8	52.4	24.3	0.4	78.5

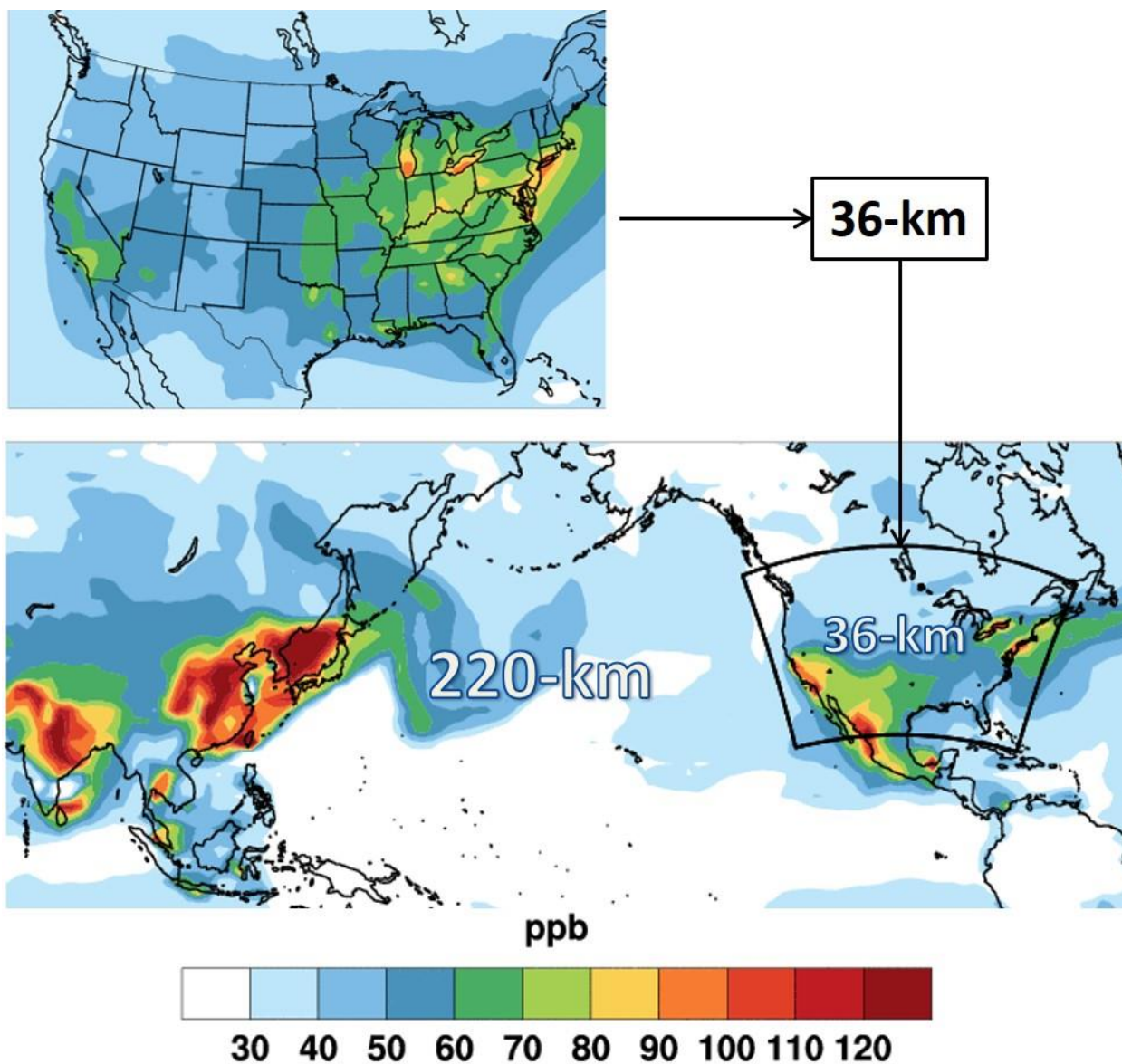


Figure 1. Projected future DM8O concentrations with future anthropogenic and biogenic emissions used to show thefor the 220-km and 36-km CMAQ modeling domains at 36 and 220-km resolutions. The 36-km modeling domain was nested inside the 220-km domain.

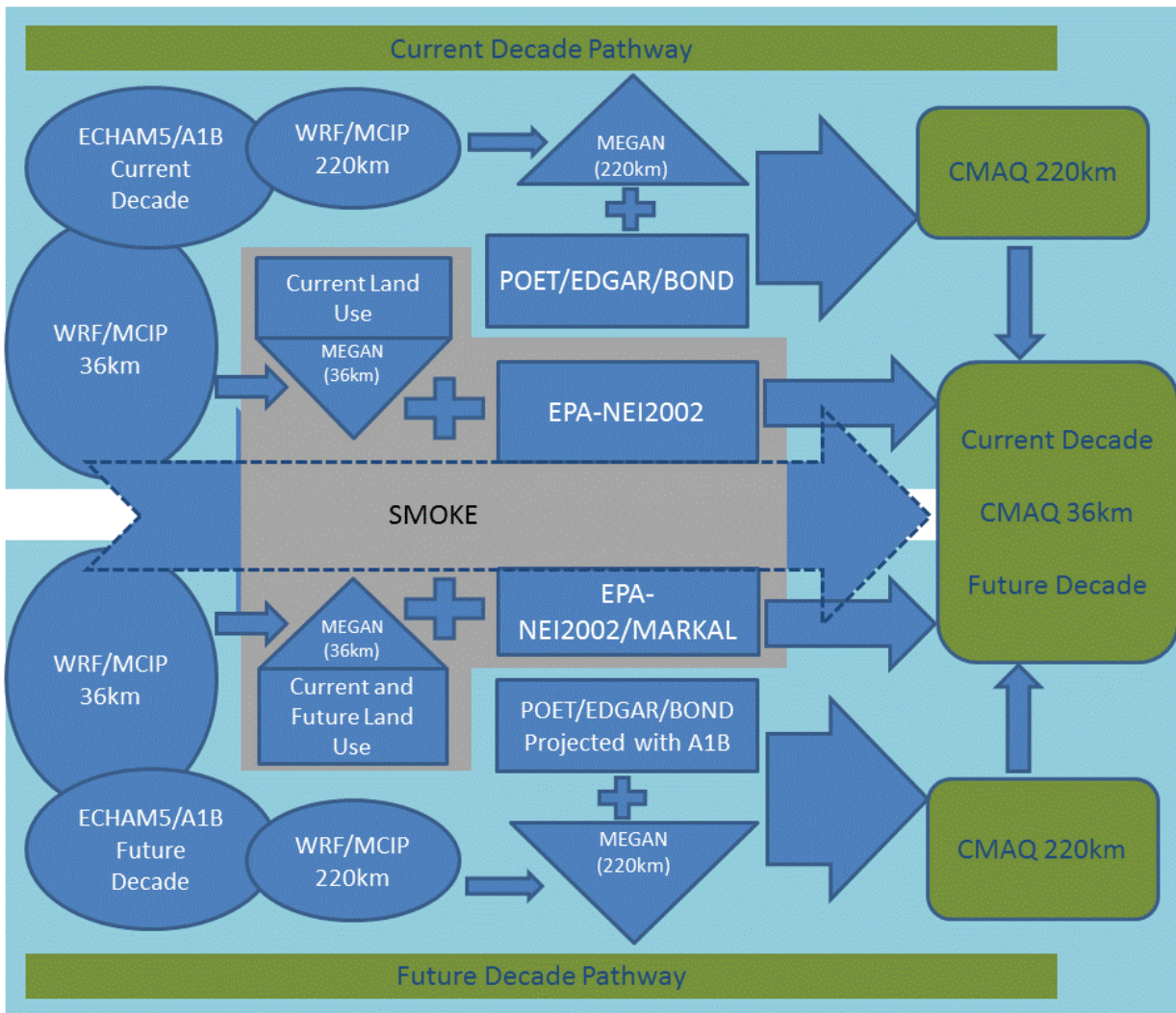


Figure 2. Schematic of the modeling framework.

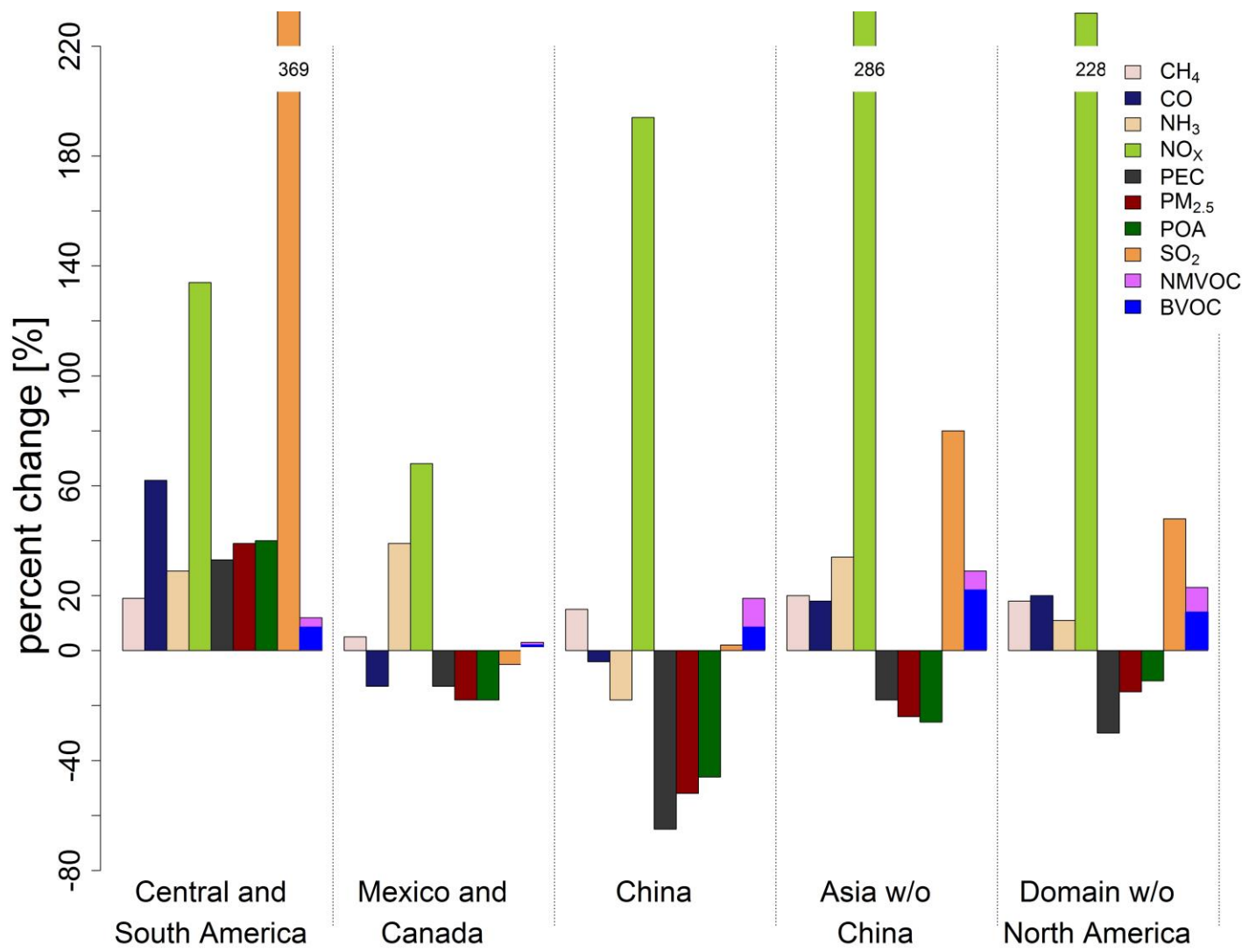


Figure 3. Summary of regional changes in global anthropogenic and biogenic emissions.

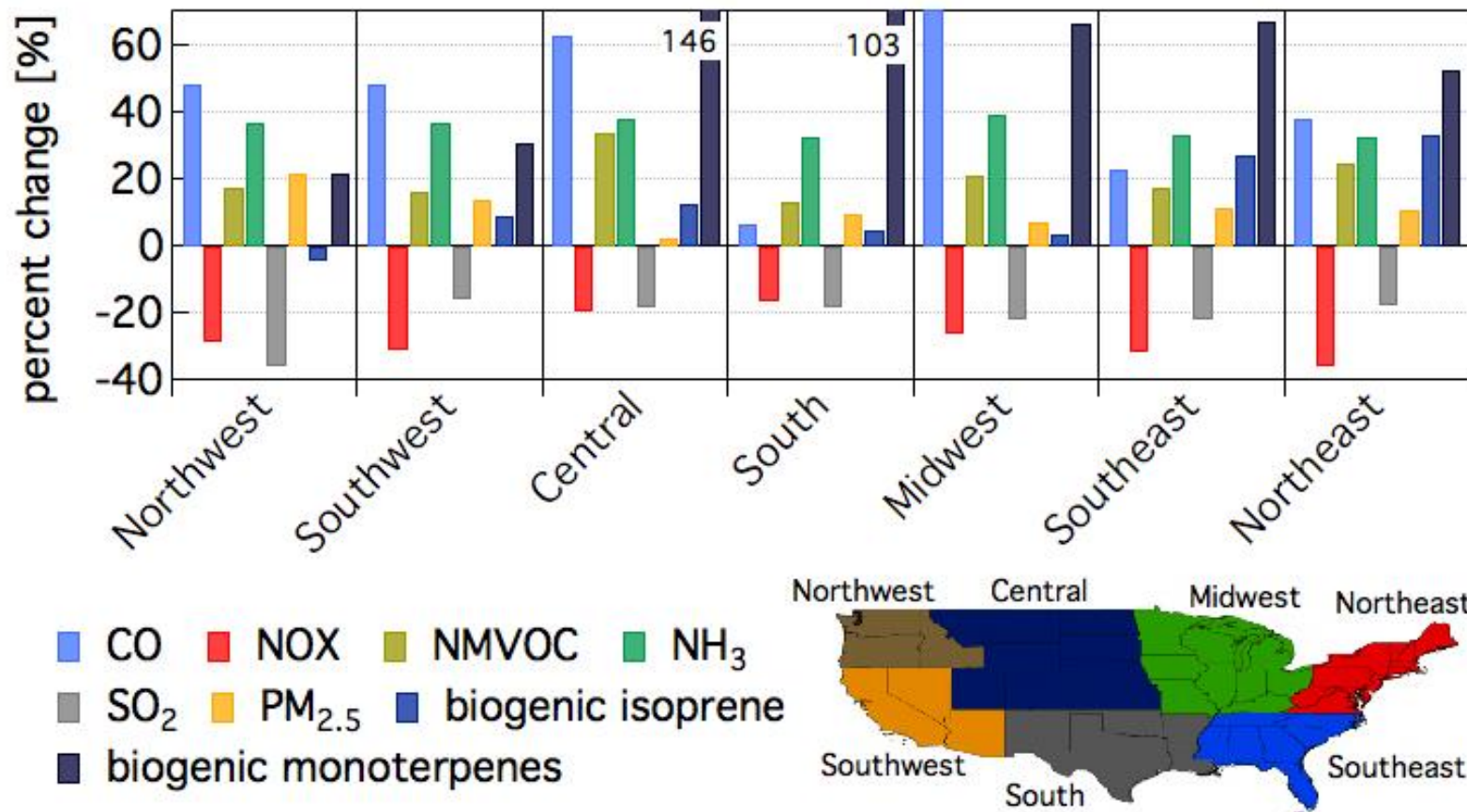


Figure 43. Summary of regional changes in US anthropogenic and biogenic emissions from future decade land use.

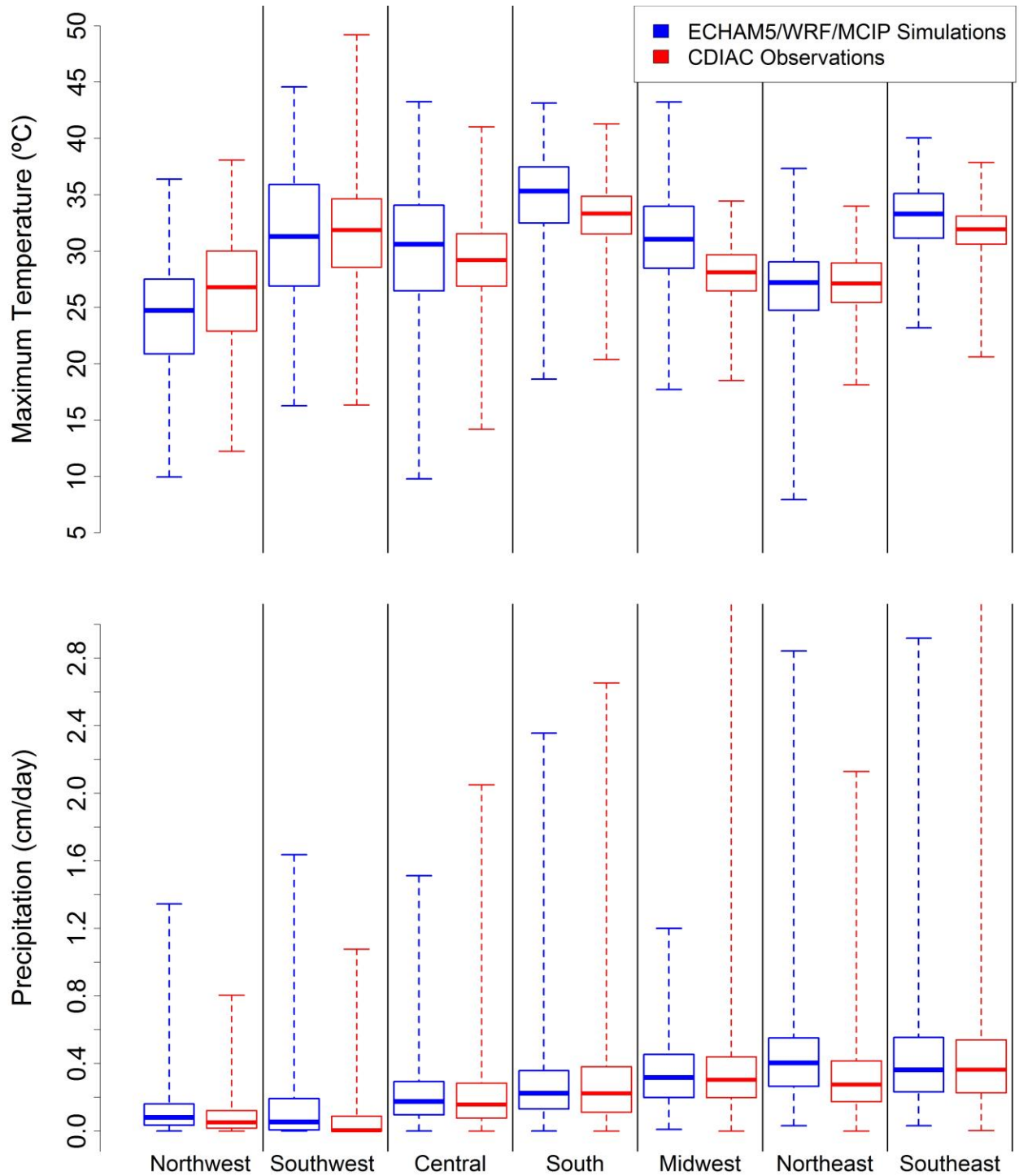


Figure 45. Comparison of modeled and observed seasonal-mean meteorological variables by region: maximum daily temperatures (top); and precipitation rates (bottom). Each box-and-whisker indicates median, 25% and 75% quartiles, maximums and minimums of the values across all sites within each region.

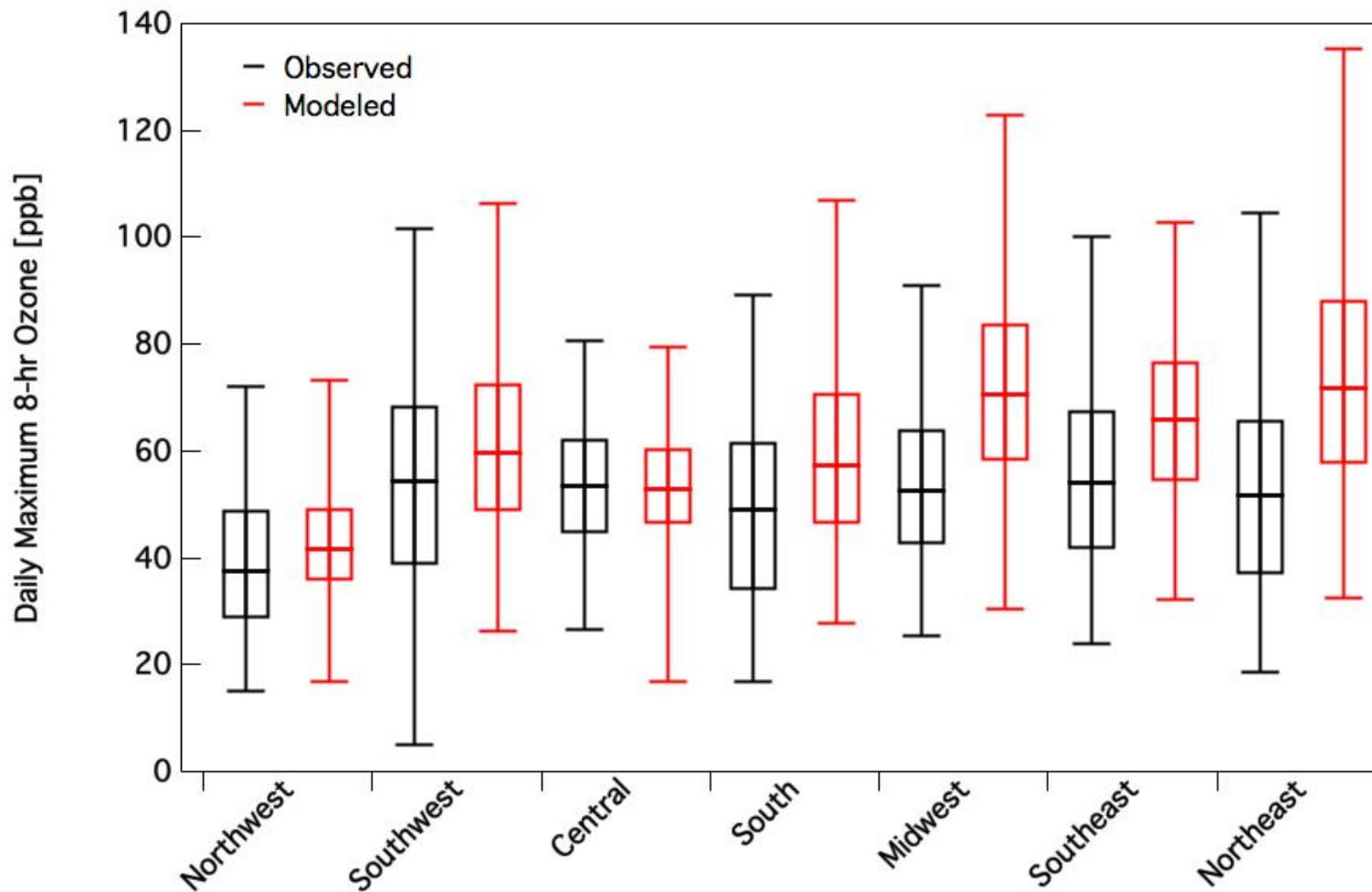


Figure 56. 2nd, 25th, 50th, 75th, 98th percentiles of observed (black) vs modeled (red) values of DM8O for each region. The number of monitoring stations per region is shown in parenthesis.

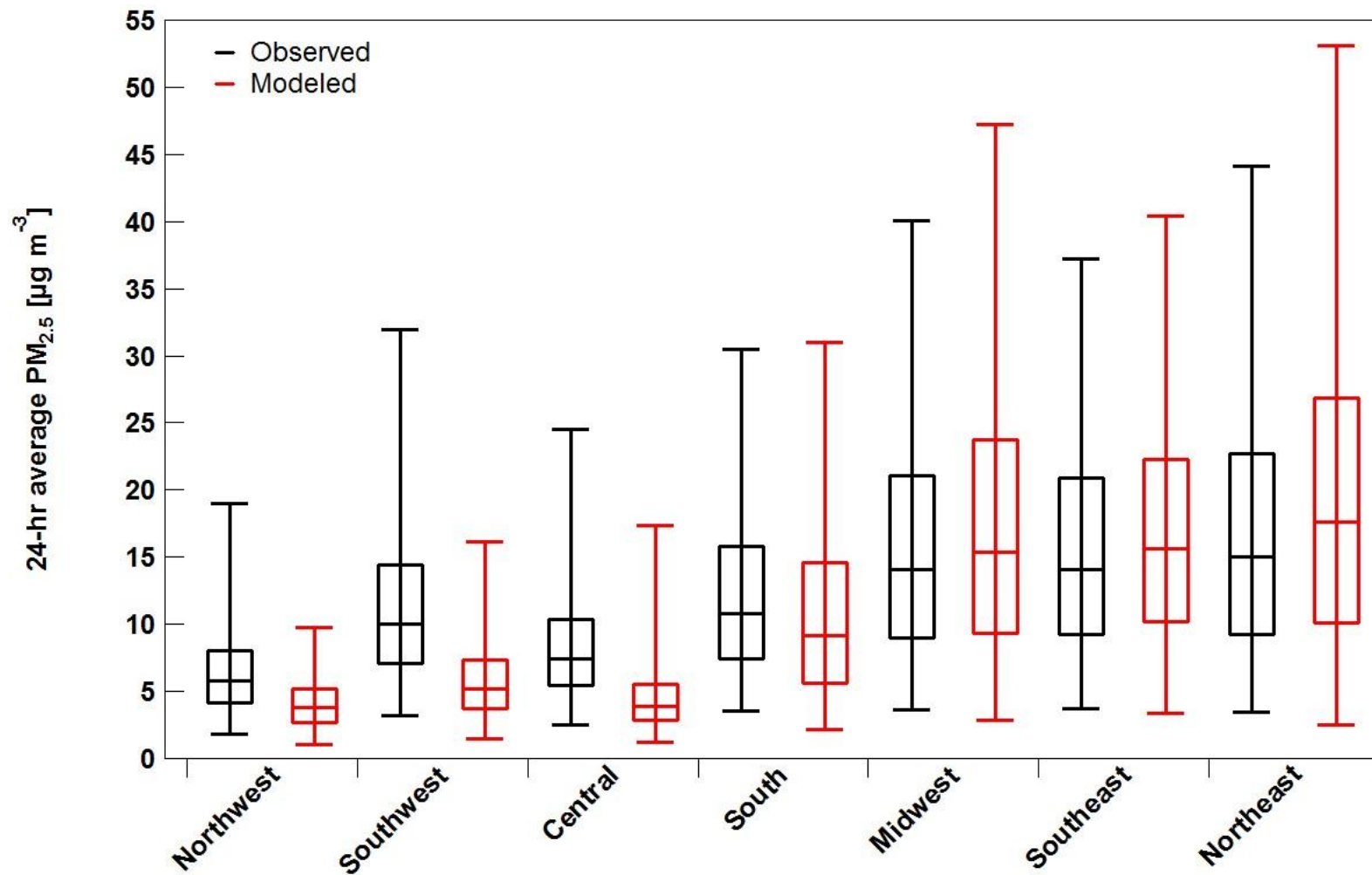


Figure 7. 2nd, 25th, 50th, 75th, 98th percentiles of observed vs modeled values of 24-hr average PM_{2.5} for each region.

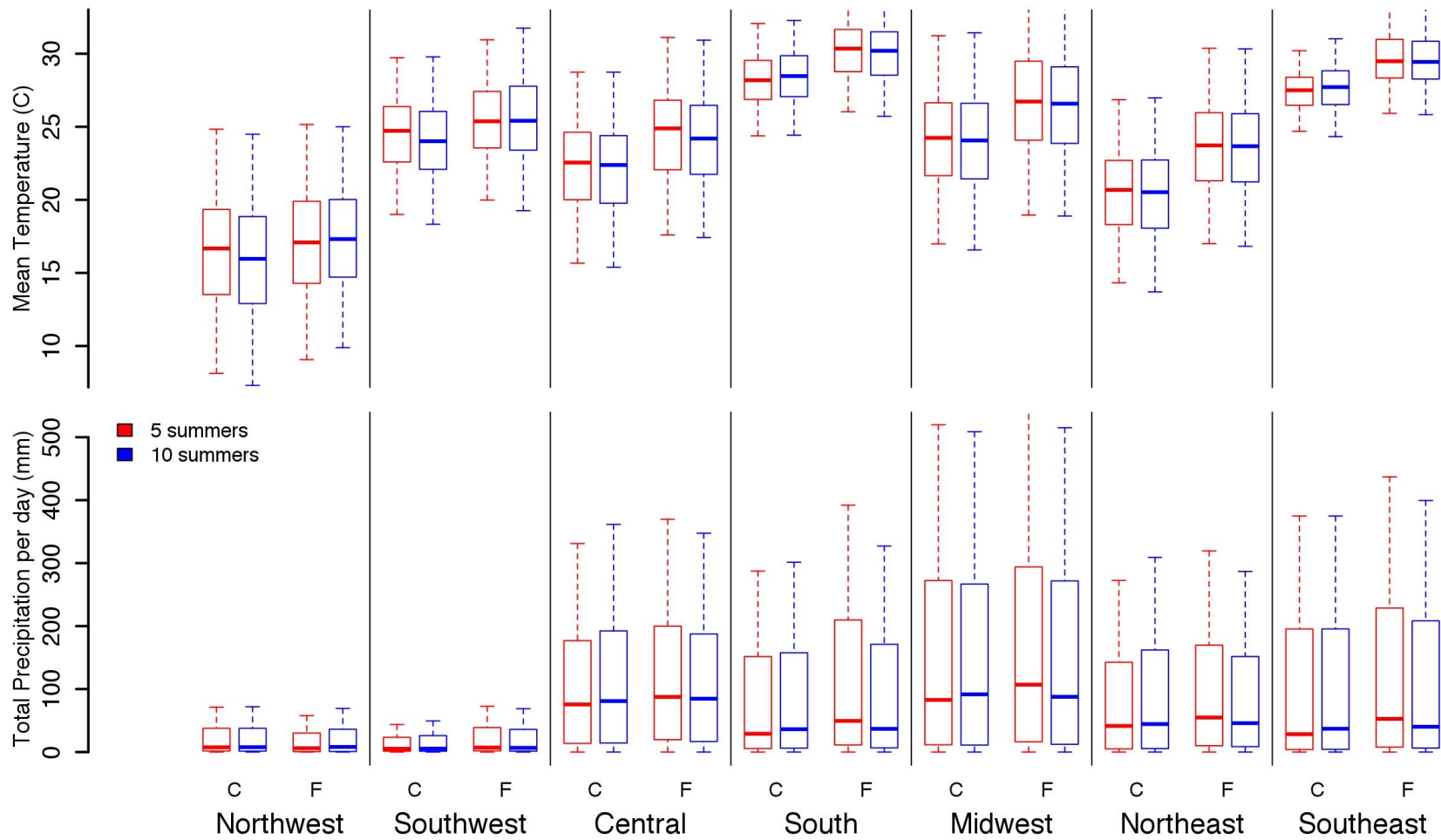


Figure 78. (Top Panel) Mean regional temperature for the five chosen summers (red) and ten summers (blue) of the current (C) and future (F) decades. (Bottom Panel) Total regional precipitation per day for the five chosen summers (red) and ten summers (blue) of the current (C) and future (F) decades. Each box-and-whisker indicates median, 5%, 25%, 75% and 95% quartiles within each region.

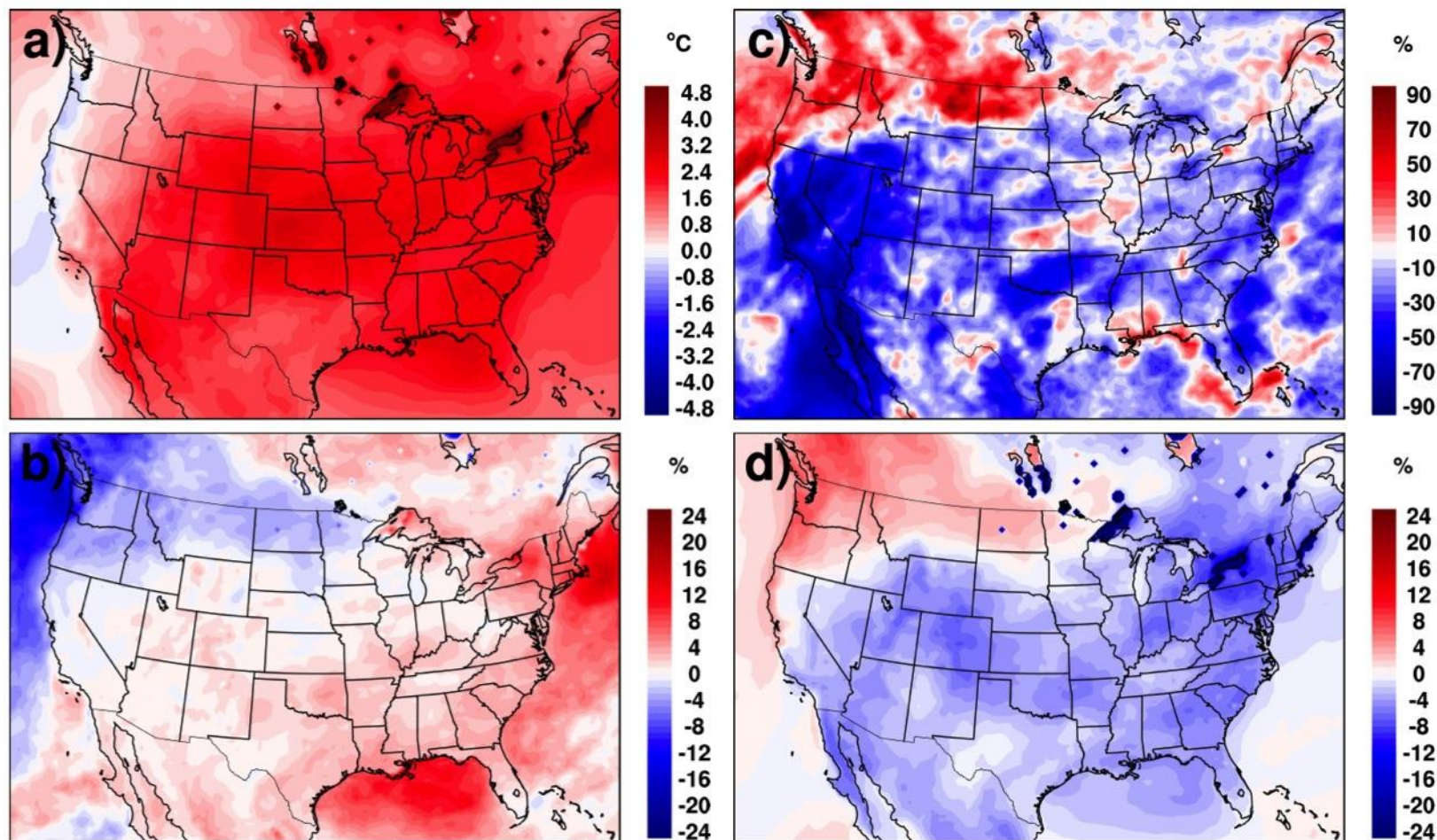


Figure 8-9 Projected changes in summertime meteorological fields (future decade - current decade): a) changes in 2-m temperature (°C); b) percent change in solar radiation reaching the ground; c) percent change in precipitation; d) change in relative humidity.

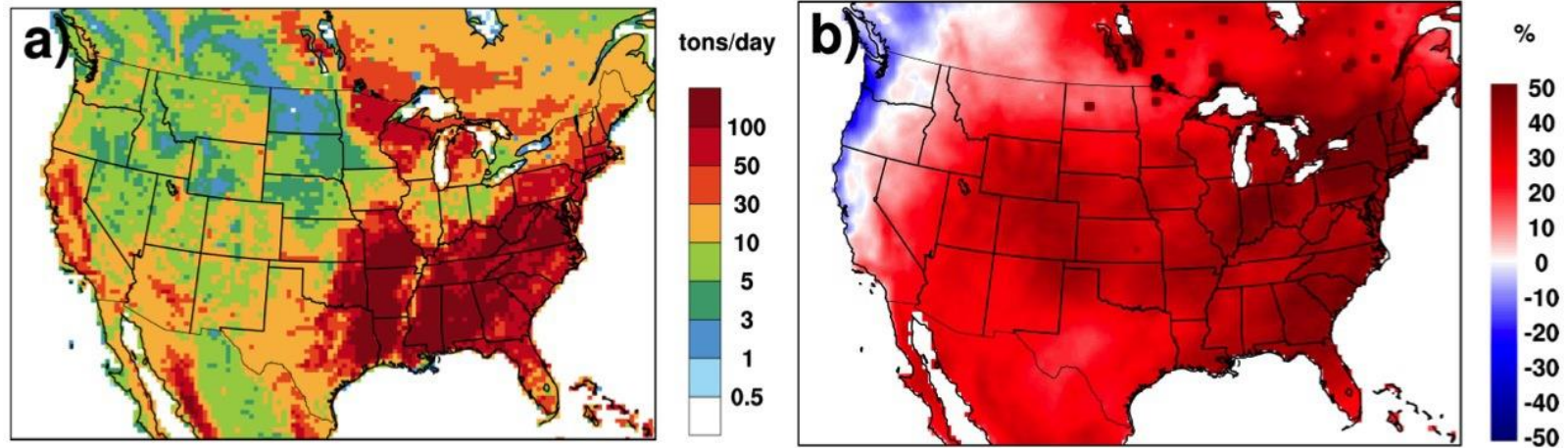


Figure 910. a) Current decade summertime isoprene emissions, and b) percent change induced by climate on future summertime isoprene emissions with current decade land use.

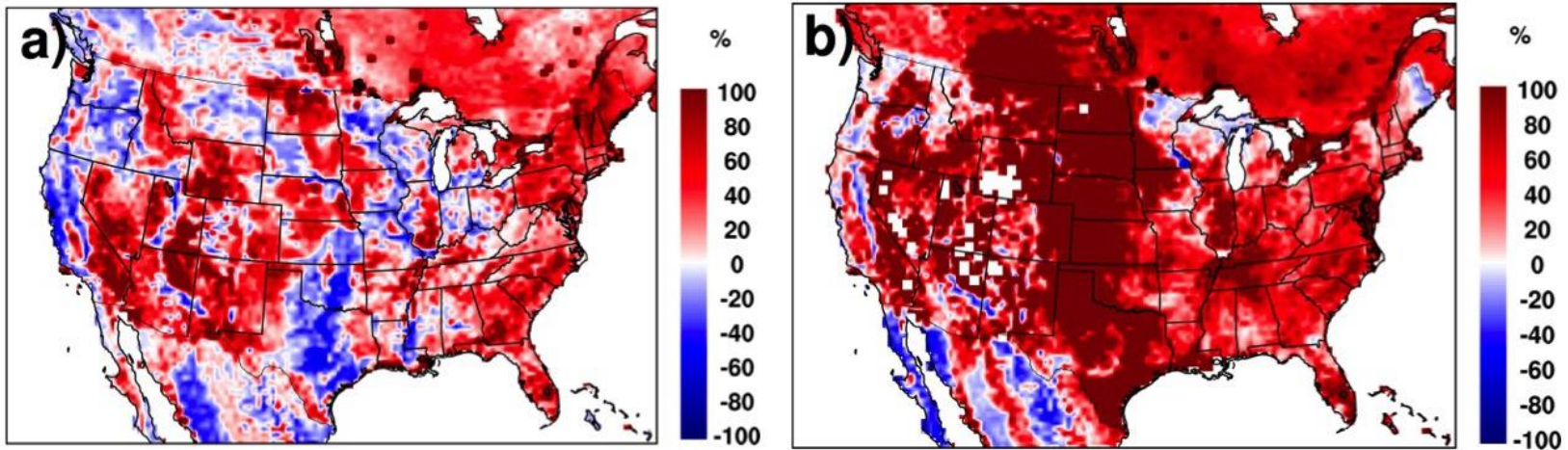


Figure 1401. Percent change between future and current decade summertime emissions for future climate and land use for a) isoprene and b) monoterpane.

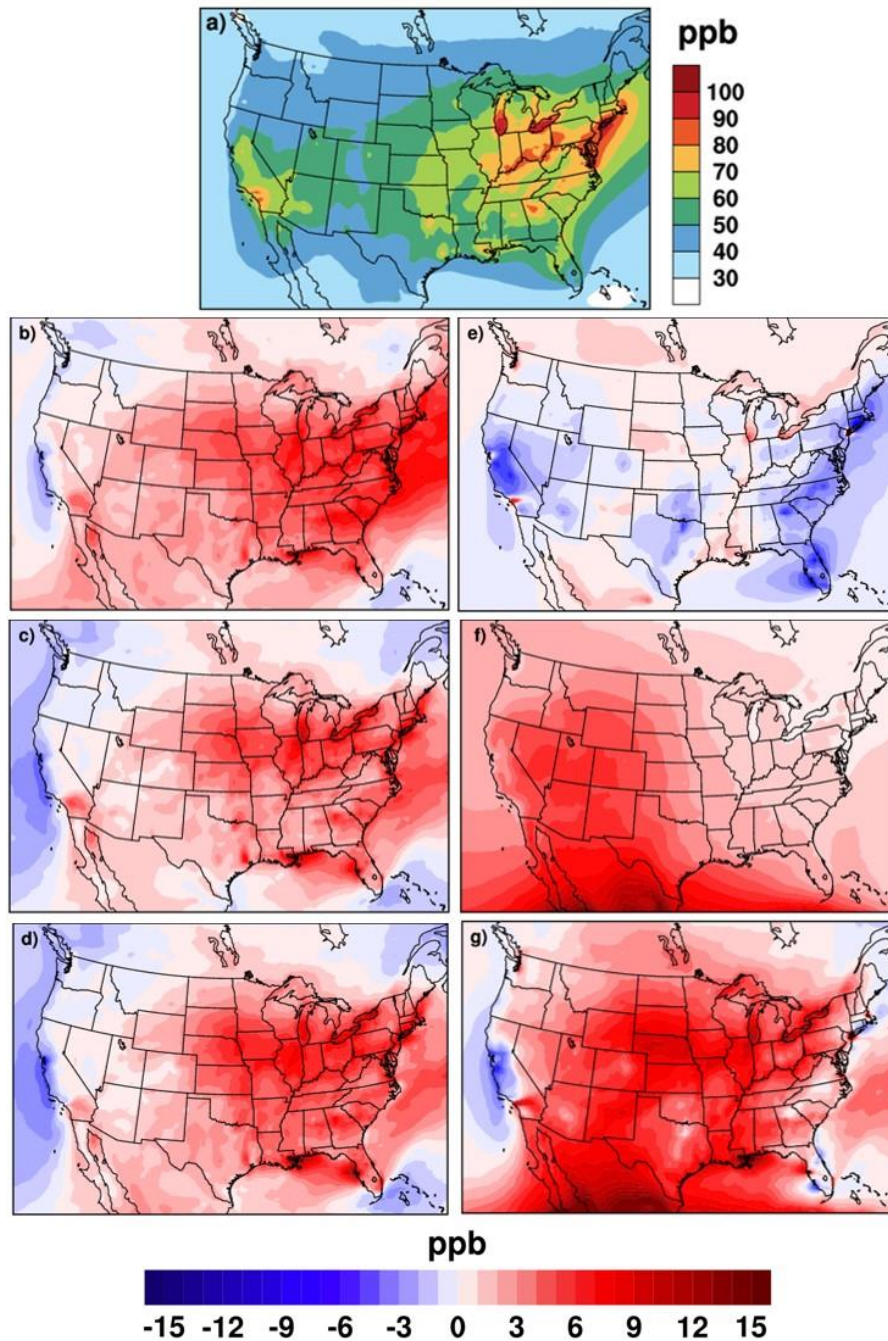


Figure 1244. a) Current decade base case daily maximum 8-hour ozone average concentrations for five summers in the 2000s; spatial distribution; and regional effect on maximum 8-hour ozone due to: b) changes in meteorology (Simulation 1 - Simulation 0); c) changes in meteorology and biogenic emissions (Simulation 2 - Simulation 0); d) changes in meteorology, biogenic emissions, and land use (Simulation 3 - Simulation 0); e) changes in US anthropogenic emissions (Simulation 4 - Simulation 0); f) changes in global anthropogenic emissions (Simulation 5 - Simulation 0); and g) all the changes above combined (Simulation 6 - Simulation 0).

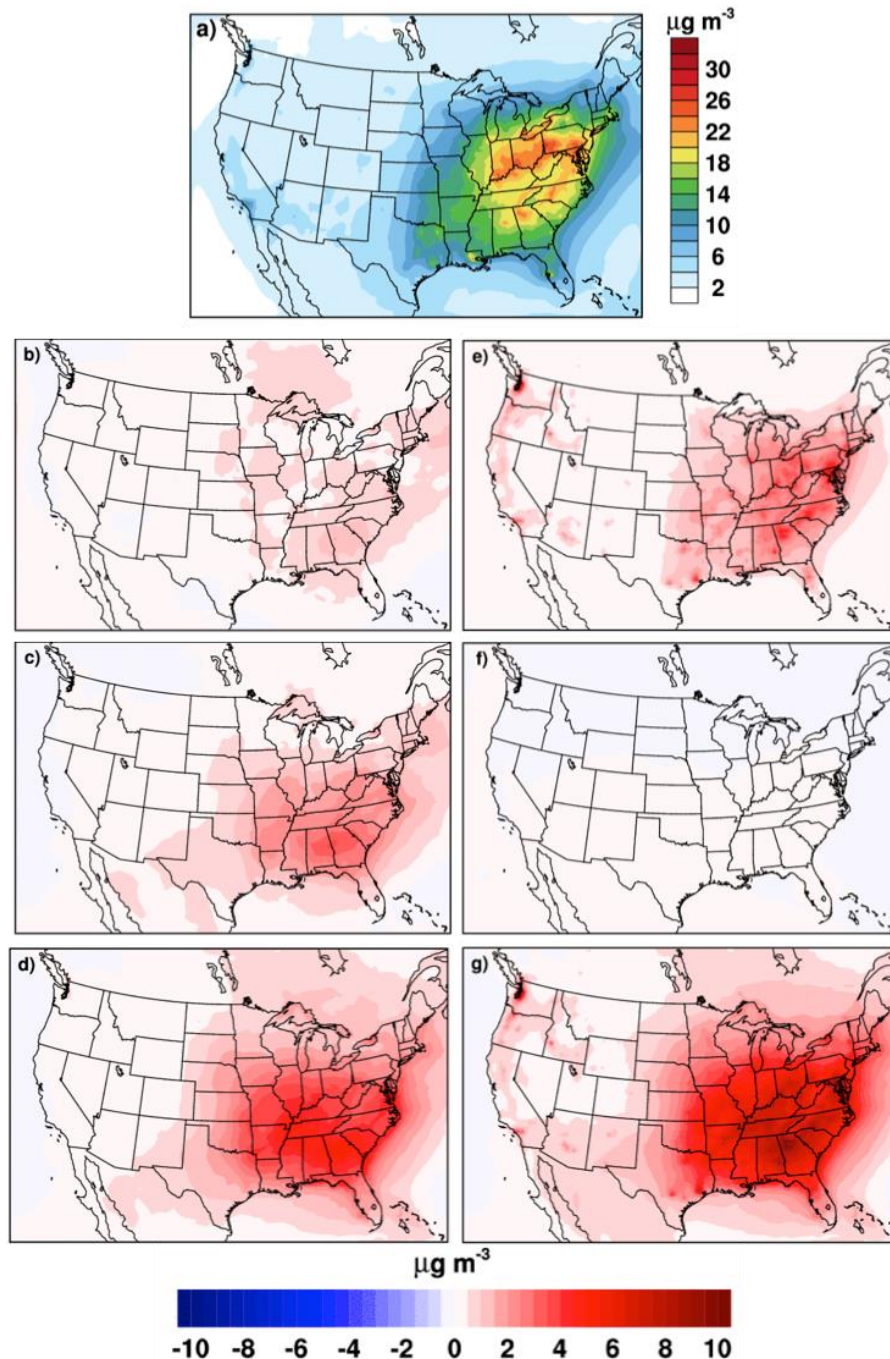


Figure 1423. a) Current decade base case PM_{2.5} average concentrations for five summers in the 2000s; and spatial distribution and regional effect on PM_{2.5} due to: b) changes in meteorology (Simulation 1 – Simulation 0); c) changes in meteorology and biogenic emissions (Simulation 2 – Simulation 0); d) changes in meteorology, biogenic emissions, and land use (Simulation 3 – Simulation 0); e) changes in US anthropogenic emissions (Simulation 4 – Simulation 0); f) changes in global anthropogenic emissions (Simulation 5 – Simulation 0); and g) all the changes above combined (Simulation 6 – Simulation 0).

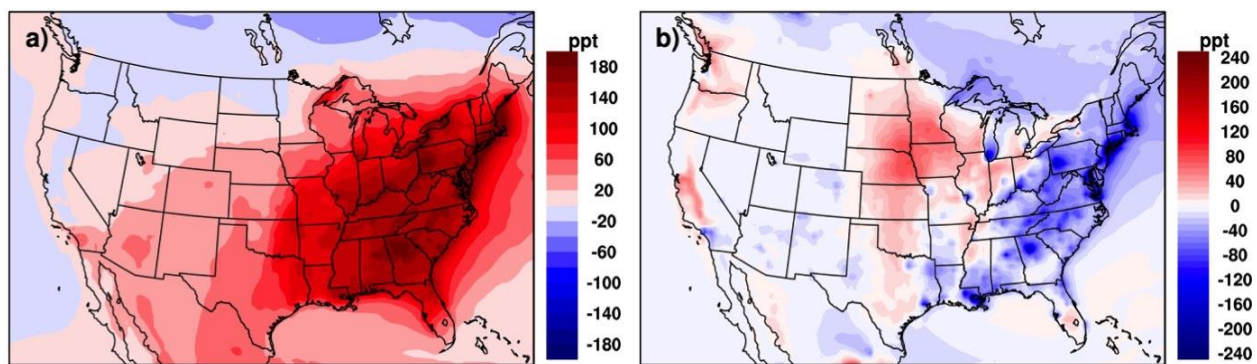


Figure 14.— Differences in (a) RNO_3 and (b) NO_x concentrations between Simulation 2 and Simulation 1.